



Evaluation of depth controller for friction stir welding of copper canisters

Lars Cederqvist

Olof Garpinger

Isak Nielsen

POSIVA OY

Olkiluoto

FI-27160 Eurajoki, Finland

Phone +358 2 8372 31

posiva.fi

SVENSK KÄRNBRÄNSLEHANTERING AB

SWEDISH NUCLEAR FUEL
AND WASTE MANAGEMENT CO

Box 3091, SE-169 03 Solna

Phone +46 8 459 84 00

skb.se

ISSN 2489-2742

Posiva SKB Report 08

SKB ID 1564157

Posiva ID RDOC-104907

June 2018

Evaluation of depth controller for friction stir welding of copper canisters

Lars Cederqvist, Svensk Kärnbränslehantering AB

Olof Garpinger, Alten AB

Isak Nielsen, IAN Consulting AB

Keywords: Friction stir welding, FSW, Automatic control.

This report concerns a study which was conducted for Svensk Kärnbränslehantering AB (SKB) and Posiva Oy. The conclusions and viewpoints presented in the report are those of the authors. SKB or Posiva may draw modified conclusions, based on additional literature sources and/or expert opinions.

A pdf version of this document can be downloaded from www.skb.se or www.posiva.fi.

© 2018 Svensk Kärnbränslehantering AB and Posiva Oy

Abstract

This study investigates the current status of the depth controller implemented on the Swedish Nuclear Fuel and Waste Management Company's (SKB) friction stir welding machine, used to develop a welding procedure to seal copper canisters containing Sweden's nuclear waste in the future. Depth control is needed to produce welds with minimum flash formation and minimum joint line hooking/remnants, which disturb the temperature control and reduce the corrosion barrier, respectively. Depth is measured using four different sensors: a Laser sensor, two linear variable differential transformers (LVDT), and an axial position sensor. The actual depth is estimated from measurements of the tool shoulder footprint and can then be compared with the depth sensor measurements. Furthermore, it is shown that copper hardness, dwell/heat-up time, and the axial force applied by the tool have the greatest influence on depth. Of these three factors, the depth controller makes use of the axial force to manipulate the shoulder depth during the first two weld sequences when the tool moves from the top of the canister's lid down to the joint line.

Thirteen welds have been carried out to verify the current status of the depth controller. The Laser sensor was used as the feedback signal to the controller, and the desired shoulder depth was set to 2.2 mm. Twelve of the thirteen welds were short and made in two different lids/rings, and one was a full circumferential weld. Flash formation was studied for each weld, and macro samples from each weld were subjected to a microscopic inspection. In addition, data from eighteen more welds (in three different lids/rings) without active depth control were collected for comparison with the depth controlled welds. The six lids used in this study varied widely in hardness, especially those used in the uncontrolled welds.

For the thirteen welds with active depth control, the shoulder depth measured by the Laser sensor varied between 2.19 and 2.40 mm (0.21 mm span) at a point two degrees into the joint line, which means a maximum control error of 0.20 mm. The LVDT sensor placed in the lid (LVDT1) had about the same variation, while the second LVDT and the axial position sensor fluctuated much more. The shoulder footprint depth ranged between 2.52–2.86 mm (0.34 mm span). For the eighteen uncontrolled welds, the Laser measurement varied between 1.74 and 2.49 mm (0.75 mm span). The corresponding range for the footprint depth was 0.60 mm. Furthermore, data from all 31 welds were used to show that, of the four depth sensors, the LVDT1 sensor is best suited for statistical modelling of the shoulder footprint depth. Additionally, the macro samples from the 13 verification welds showed no signs of joint line hooking or remnants. The flash formations during the same welds were also minimal (0–1 mm).

It was concluded that the LVDT1 sensor is best suited for feedback to the depth controller since it is the best of the four depth sensors at modelling the shoulder footprint depth and because, unlike the Laser sensor, it does not suffer from extensive measurement noise. The depths of the controlled welds varied roughly half as much as those of the uncontrolled welds. It remains to be investigated whether the varying copper hardness is a factor or if the wider depth range was the result of the depth control alone. An option to the current depth control strategy might be to employ depth control during the dwell sequence. The heat-up time could then be varied as a complement to the axial force manipulation in the depth controller. In addition, it is also recommended that a fail-safe system be implemented for the depth controller. In the case of a sensor failure, this system would automatically switch the depth measurement signal that is fed back to the depth controller.

Sammanfattning

Denna studie undersöker nuvarande status för djupregulatorn som är implementerad på SKB:s svetsmaskin. På SKB:s kapsellaboratorium utvecklas en svetsprocedur för att försluta 5 cm tjocka kopparkapslar innehållandes Sveriges använda kärnbränsle, och svetsmetoden som används är friktionsomrörningssvetsning (FSW, eng. Friction stir welding). Djupreglering behövs för att producera svetsar utan eller med minimalt så kallat svetseskägg och med minimal rotdiskontinuitet (så kallad foglinjesböjning eller kvarvarande fog). Svetseskägg stör temperaturreglering (främst vid den så kallade överlappssekvensen) och rotdiskontinuiteter minskar korrosionsbarriären. Djupet mäts med fyra olika sensorer; en laser, två lägesgivare och en axiell positionsgivare. Det verkliga djupet uppskattas från mätning av den konvexa verktygsskuldrans spårbredd och jämförs sedan med sensorerna. Studien visar att hårdheten på kopparen, uppvärmningstid och svetsverktygets axiella kraft har störst inverkan på djupet. Av dessa tre faktorer justerar djupregulatorn den axiella kraften för att styra skulderdjupet under de två första svetssekvenserna när verktyget rör sig från startpositionen, högt upp i locket, ner till foglinjen.

Tretton svetsar har genomförts för att verifiera djupregulatorns nuvarande status. Lasersensorn användes som återkopplingssignal till regulatorn, och det önskade skulderdjupet sattes till 2,2 mm. Tolv av de tretton svetsarna var korta och gjordes i två olika lock/rörringar, och en av svetsarna var en fullvarvssvets. Skäggbildningen mätes vid alla svetsar, och makroprov från alla svetsar togs ut för att analysera eventuella rotdiskontinuiteter. Dessutom används data från ytterligare arton svetsar (från tre lock/rörringar) som gjorts utan djupreglering, för jämförelse. De sex lock som använts i denna studie varierar kraftigt i hårdhet, speciellt de lock som användes för svetsar utan djupreglering.

För de tretton svetsarna med djupreglering så varierade skulderdjupet, mätt med lasersensorn, mellan 2,19 och 2,40 mm vid en position 2 grader in i foglinjesekvensen, vilket motsvarar ett maximalt reglerfel på 0,20 mm. Lägesgivaren placerad i locket (benämns LVDT1) hade ungefär samma variation, medan den andra lägesgivaren och axiella positionsgivaren varierade mycket mer. Det uträknade djupet från skuldrans spårbredd varierade 0,34 mm, mellan 2,52 och 2,86 mm. Vid de arton svetsarna utan djupreglering varierade lasersensorn 0,75 mm, mellan 1,74 och 2,49 mm. Den motsvarande variationen för spårbredden var 0,60 mm. Dessutom visar data från alla 31 svetsar att av de fyra djupsensorerna så är LVDT1 bäst lämpad för statistisk modellering av skuldrans spårbreddsdjup. Vidare visar makroprov från de 13 svetsarna med djupreglering inga rotdiskontinuiteter, varken foglinjesböjning eller kvarvarande fog. Skäggbildningen under dessa svetsar var också minimal, mellan 0 och 1 mm.

Slutsatsen är att LVDT1-sensorn är bäst lämpad för återkoppling till djupregulatorn då den är bästa av de fyra sensorerna att modellera skuldrans spårbreddsdjup och eftersom den, till skillnad från laser-sensorn, inte lider av omfattande mätbrus. Djupet för svetsarna med djupreglering varierade ungefär hälften så mycket som för svetsarna utan djupreglering. Det återstår att undersöka om den varierande hårdheten på locken är en faktor eller om den större djupvariationen vid svetsar utan djupregleringen endast beror på avsaknaden av reglering. Ett komplement till den nuvarande djupregleringsstrategin skulle kunna vara att även använda djupreglering under uppvärmningssekvensen. Uppvärmningstiden skulle då kunna varieras för att underlätta för djupregleringen. Dessutom rekommenderas att ett felsäkert system implementeras så att sensorsignalen byts ifall det blir fel på den sensor som används av regulatorn.

Contents

1	Introduction	7
1.1	Background	7
1.2	Friction stir welding	7
1.3	Weld machine description	8
1.4	The weld cycle	8
1.5	Temperature control of the FSW process	10
1.6	Motivation of the depth controller	11
1.7	Depth sensor and other depth indicators	12
	1.7.1 Axis Z position sensor	12
	1.7.2 Laser sensor	13
	1.7.3 LVDT sensors	14
	1.7.4 Shoulder outer diameter temperature	15
1.8	Measures of the actual depth	16
2	Factors that influence depth	17
2.1	Hardness	17
2.2	Heat-up time, total power input, and transition temperatures	18
2.3	Axial force	20
3	The depth controller	21
3.1	Automatic control	21
3.2	The PID controller	21
3.3	Depth controller	21
4	Questions for the report to answer	23
5	Depth controller verification welds	25
5.1	Results from the verification welds	25
5.2	Results from the macro sample tests	32
6	Comparison with welds without depth control	35
7	Conclusions	43
	References	45

1 Introduction

The main purpose of this report is to present the current depth controller, its status, and future plans for the depth control process. The first chapter gives a background on friction stir welding (FSW) in general and SKB's application of FSW in particular. Chapter two provides an overview of factors that affect the resulting depth and how those factors can be controlled. The third chapter gives a background on automatic control, as well as on PID controllers, and presents the depth controller that is currently implemented on the welding machine. Chapter four identifies a number of important questions for this report to answer, while the fifth chapter presents the welds used for depth verification and their results. In the sixth chapter, these welds are compared to a number of welds made without any active depth control to see if there are any clear benefits to the use of the controller. Several models for the shoulder footprint are also presented in chapter six, and the benefits of the different sensors are compared. The seventh and last chapter concludes the report and answers the questions posed in chapter four.

1.1 Background

The Swedish Nuclear Fuel and Waste Management Company (SKB) plans to join at least 12 000 lids and bases to the extruded copper tubes containing Sweden's nuclear waste, using FSW as described by Thegerström (2004). The canisters thus produced (5 m height, 1 m diameter) are a major component of the Swedish system for managing and disposing of radioactive waste. They will be stored in the Swedish bedrock and must remain intact for 100 000 years. A corrosion barrier of 5 cm thick copper and a cast iron insert for mechanical strength are used to meet this requirement. To ensure that safe, high quality welds are produced repeatedly during more than 40 years of production, the FSW process needs automatic control. This report addresses the depth control portion of the machine's automatic control system.

1.2 Friction stir welding

FSW is a thermo-mechanical, solid-state process invented in 1991 at The Welding Institute (TWI) in Cambridge, England (Thomas et al. 1991). A rotating, non-consumable tool, consisting of a tapered probe and shoulder (the shoulder has a convex shape for SKB's application), is plunged into the metal to be welded and traverses along the joint line, see Figure 1-1. For thick section welds (like the copper canisters), a pilot hole is drilled before the actual weld, to reduce probe wear. Frictional heat is generated between the tool and the metal being welded, causing the metal to soften without reaching the melting point, and allowing the tool to traverse the joint line.

Friction stir welding typically has three weld parameters (see Figure 1-1), namely:

1. Tool rotation rate (rpm).
2. Tool traverse speed (mm/min).
3. Axial force (kN).

The axial force is also called the Z-force, as it is applied along the machine's Z-axis. For the purposes of monitoring and providing feedback to the controller, several machine variables are measured on SKB's FSW process. The most important ones include:

1. Tool temperature (°C).
2. Spindle torque (Nm) required to maintain the desired tool rotation rate.
3. Shoulder depth (mm) into the welded material.

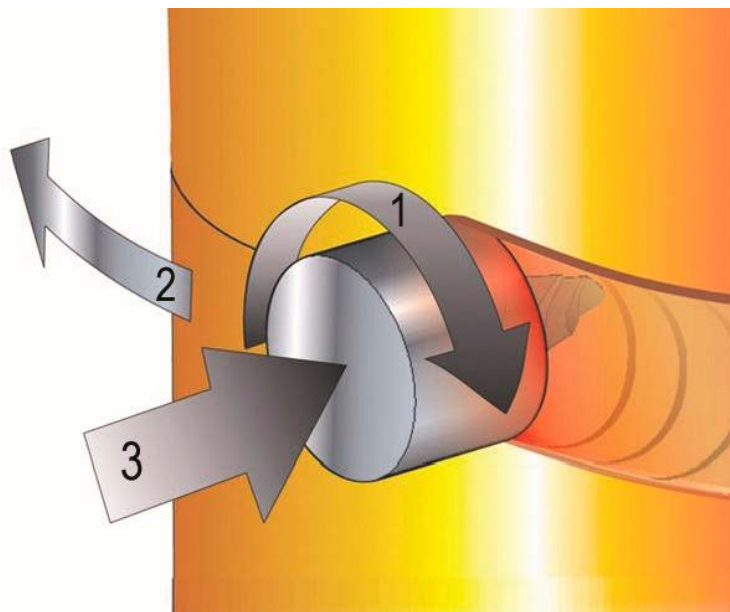


Figure 1-1. Illustration of the friction stir welding process and the three weld parameters: 1. Tool rotation rate, 2. Tool traverse speed, 3. Axial force.

There are some important elementary relationships between these variables. The tool rotation rate multiplied by the torque and divided by the traverse speed is equal to the heat input in units of kJ/mm. Since the traverse speed is kept constant during welds in this study, the power input (measured in kW), which is the tool rotation rate multiplied by the spindle torque, is used instead. Both quantities are closely correlated to the tool temperature (Cederqvist 2011).

1.3 Weld machine description

In 2003, a purpose-built machine from ESAB was installed at SKB's Canister laboratory in Oskarshamn (see Figure 1-2). In this machine, the welding head rotates up to 425 degrees around the canister, which is clamped with a force of 3200 kN. The lid is pressed down with a force of 400 kN. To achieve a weld zone with minimal oxide inclusions, an argon gas shield is placed over the entire weld region.

1.4 The weld cycle

Prior to the weld, a hole is drilled in the lid to prepare for the pilot hole. A different probe than the one used in the actual weld is then used to form a conical pilot hole, which will reduce stress on the probe used for welding.

In terms of constant thermal boundary conditions and controller requirements, the simplest weld cycle is a weld that starts and ends at the joint line. However, since a probe-shaped exit-hole is left when the tool is retracted, the weld cycle needs to end above the joint line, where it will not affect the 5 cm thick corrosion barrier. In addition, the weld is started above the joint line to further reduce the risk of defect formation at the joint line. This also makes it possible to abort the process should anything go wrong during start-up. Another weld will then be made in a new pilot hole, rather than rejecting the canister.

A full circumferential weld can be divided into five different sequences, as illustrated in Figure 1-3. These sequences are:

1. *The dwell sequence*, used to raise the welding temperature to the point where the copper softens, allowing the tool to start its traversal.
2. *The start sequence*, in which the tool is accelerated to a constant traverse speed and run until a specified welding temperature is reached.
3. *The downward sequence*, where the tool moves down to the joint line.
4. *The joint line sequence*, in which the tool runs along the joint for 360 degrees. The last part (approximately 15 degrees) of the joint line sequence is called the overlap sequence since the tool overlaps the initial joint line sequence.
5. *The parking sequence*, where the tool moves back into the lid, to be withdrawn.



Figure 1-2. Purpose-built FSW machine for copper canister welding, before the argon gas shield was installed.

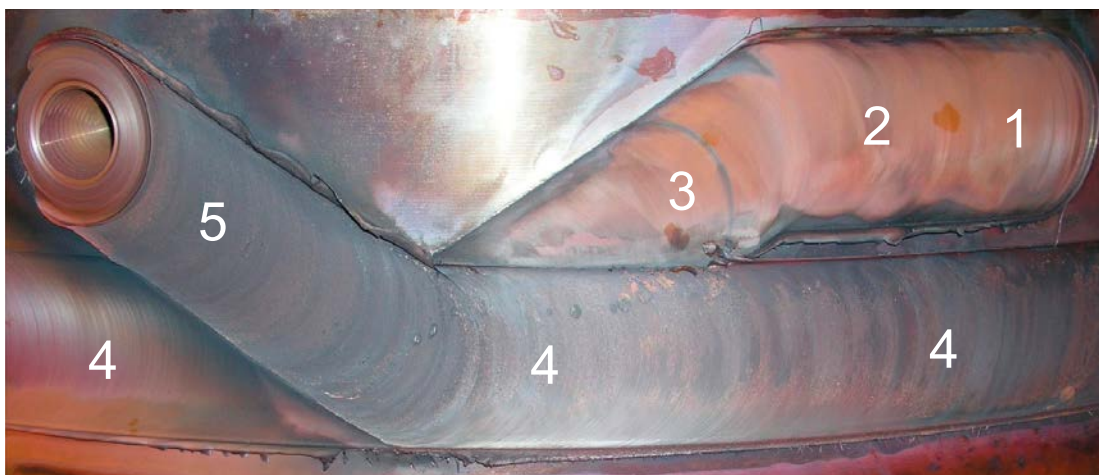


Figure 1-3. Sequences during a full weld cycle.

The different sequences in the weld cycle result in non-uniform thermal boundary conditions throughout the weld. As a consequence, the input power needed to keep the welding temperature within the process window throughout the 45 minute long weld cycle varies.

Since full lap welds are expensive to make, shorter welds are often used to evaluate weld performance. Such welds typically include sequences 1–4, where the joint line sequence is much shorter than 360 degrees. This way, a lid is normally divided into at least six shorter welds.

1.5 Temperature control of the FSW process

Measuring the welding temperature is not a trivial matter. The sensors (thermocouples) are placed in the welding tool and should ideally be placed to best correlate with weld quality. Figure 1-4 shows the welding tool in profile and the locations of the three thermocouples currently used to measure the welding temperature (ID and OD stands for Inner and Outer Diameter, respectively).

If the welding temperature gets too high for an extended period of time, there is a risk of probe fracture (has occurred at probe temperatures above 910 °C), resulting in a rejected canister, requiring both extensive and expensive work to remove the nuclear waste. Similarly, temperatures that are too low may result in discontinuities in the weld (known as wormholes) that could, depending on size, also lead to a rejected canister. Due to varying thermal boundary conditions throughout the weld cycle, it is necessary to use automatic temperature control. The current solution includes a cascade controller with an inner power input controller, which handles fast torque disturbances and an outer temperature controller that addresses slower temperature disturbances (Cederqvist et al. 2012a). It has been shown that the probe temperature is best correlated with weld quality, and therefore probe temperature is used by the controller (Cederqvist 2011). The desired (reference) probe temperature is set to 845 °C, which is considered safe with respect to both discontinuities and probe fractures (Cederqvist 2011). The temperature controller is usually able to keep the temperature within ± 5 °C of this reference value during the entire joint line sequence, which is well within the normal window for good quality welds. A safety system has also been implemented to use back-up temperature control strategies in case one or more of the sensors used by the temperature controller malfunctions during a weld.

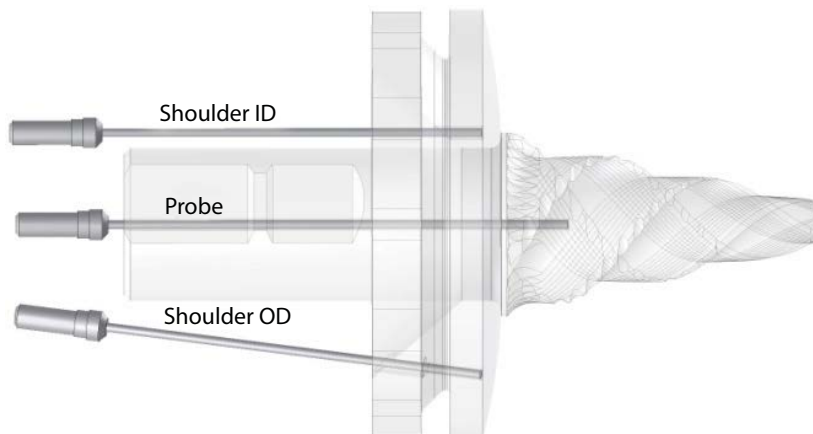


Figure 1-4. Thermocouple placements in the weld tool.

1.6 Motivation of the depth controller

In this report, depth will be defined as the extent to which the convex shoulder penetrates the copper surface. This is also called the shoulder depth in this report, and it should be noted that the convex part of the shoulder used has a depth of 3 mm. By adding the probe length to the shoulder depth, one can calculate the total depth of penetration of the tool. Currently a probe length of 51 mm is standard, but most probes are used in more than one weld, and experience has shown that the probe length will decrease by approximately 0.1–0.3 mm/weld (for short welds).

There are two important weld criteria associated with depth that increase the importance of depth control throughout the weld:

1. Maximizing the corrosion barrier by minimizing joint line hooking or any remaining joint line.
2. Avoiding large torque disturbances caused by flash formation at the overlap sequence.

An ideal weld has little to no flash (see Figure 1-5a), and the tip of the tool just barely reaches the vertical joint line (see Figure 1-6a). If a weld is too shallow, it results in a joint line remnant (see Figure 1-6b), which decreases the corrosion barrier. Deep welds, on the other hand, lead to extensive flash (see Figure 1-5b) and leave a joint line hooking defect (see Figure 1-6c), which also decreases the corrosion barrier. Flash during the downward sequence typically leads to a quick torque decrease (disturbance) at the overlap sequence. Such a disturbance usually reduces the shoulder ID and OD temperatures, but not the controlled probe temperature. Since the temperature controller reacts to the torque disturbance by increasing the tool rotation rate, this results in a probe temperature increase of approximately 5–10 °C. It is thus desired to get as little flash formation as possible during the downward sequence and the beginning of the joint line sequence.

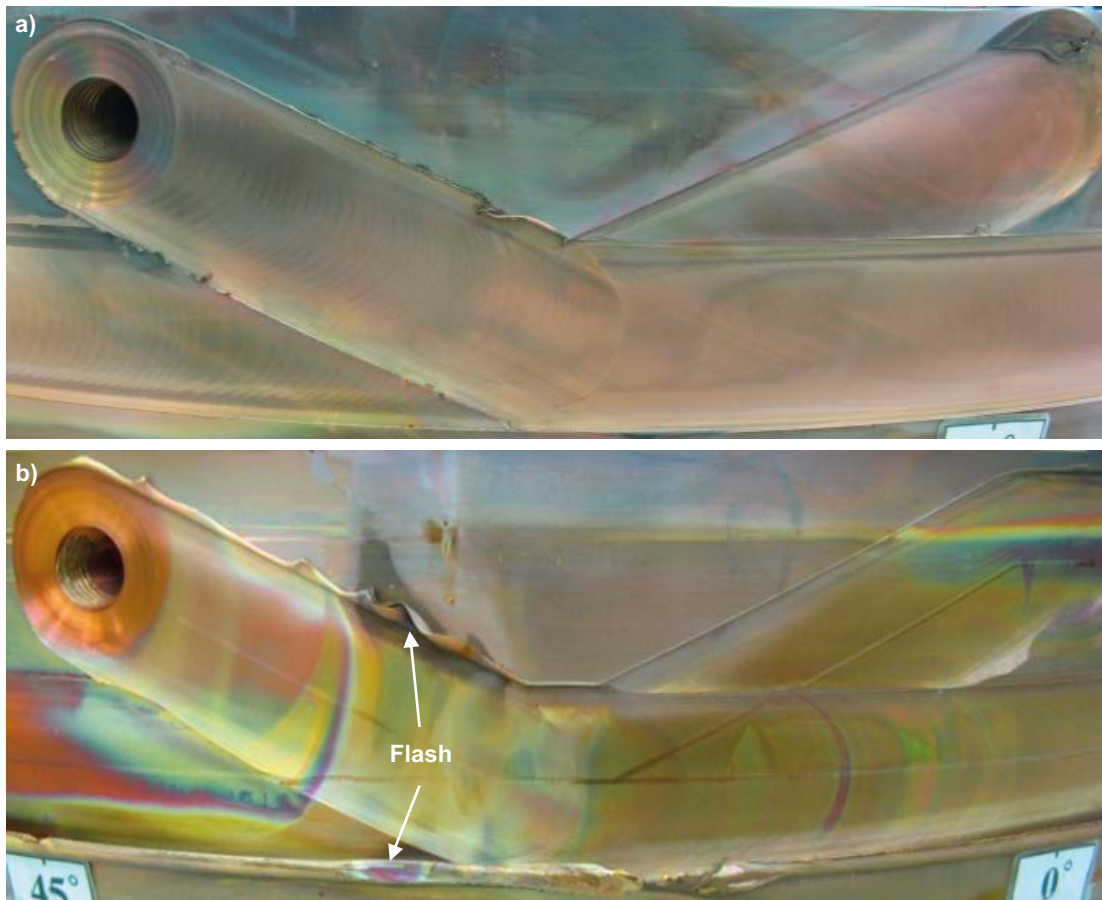


Figure 1-5. a) Weld with little flash, mainly occurring during the parking sequence. b) Weld with extensive flash formation during joint line and parking sequences.

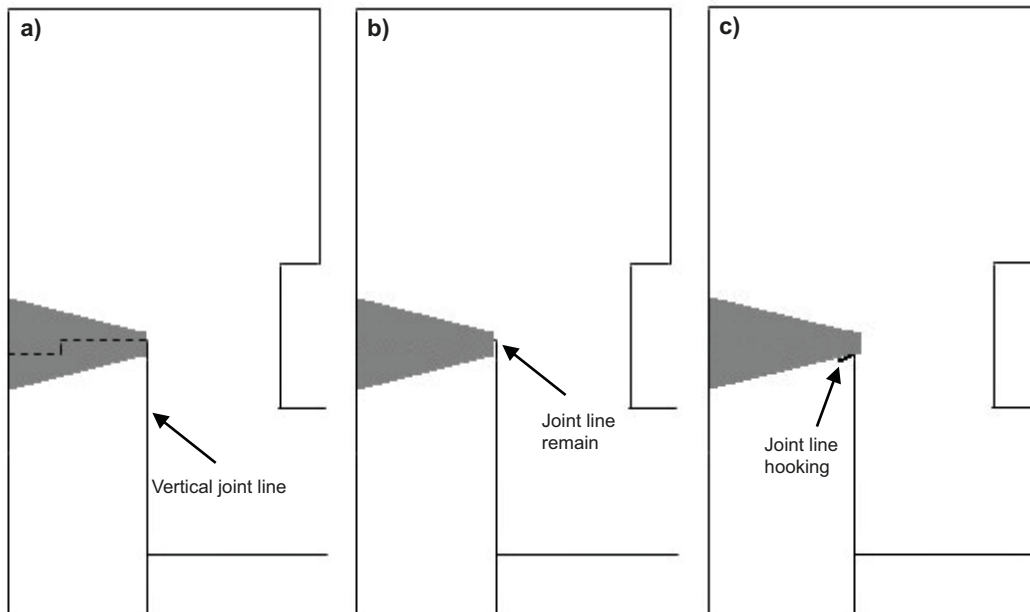


Figure 1-6. a) Ideal weld where the tool tip just barely reaches the vertical joint line. b) Shallow weld that leaves a remnant of the joint line c) Deep weld that leads to joint line hooking.

1.7 Depth sensor and other depth indicators

There are currently four depth sensors attached to the FSW machine:

1. Axis Z position sensor.
2. Laser sensor.
3. Two linear variable differential transformer (LVDT) sensors, called LVDT1 and LVDT2.

1.7.1 Axis Z position sensor

The Axis Z position sensor measures the position of the tool in relation to the gear rim to which the Z-axis is attached, see Figure 1-7. This is the most commonly used measure of FSW depth, but it has a number of shortcomings, especially for SKB's canister sealing. The sensor measurements hold a combination of information about:

1. *Depth* (the information that needs to be extracted).
2. *Thermal expansion*. The higher the temperature is, the greater the thermal expansion, thus resulting in an apparently shallow depth measure. The expansion is quite challenging to predict, and currently it is assumed to be more or less reproducible between welds, since the probe temperature is controlled to the same magnitude for each weld.
3. *Canister eccentricity and inclination*. The canister is never mounted entirely centred and straight, typically adding a skewed sine wave to the measurements of 360 degree welds. A ball bearing tool (BBT) (see Figure 1-8) is used to traverse the canister surface (using constant low Z-force) to map this effect on the data, but such a model is not currently used by the controller.
4. *Canister movement*. BBT-data from before and after the welds indicate that the canister moves slightly during welding. This movement will cause an effect similar to that of canister eccentricity and inclination and could thus ruin their estimation. It is not modelled for the FSW machine.
5. *Axis Z deflection*. The Z-axis is not completely stiff, which means that it will flex under loading and thus indicate greater depth than it should. This effect has been modelled and is subtracted from the actual Axis Z position value.
6. *Variations in the gear rim shape*. The gear rim around which the Z-axis moves will never be perfectly circular and will thus result in a relatively repeatable pattern in the depth measurements. This effect has been modelled and is subtracted from the actual Axis Z position value.

All in all, there are up to five different possible sources of misinformation in the Axis Z position signal, which make it very difficult to use the Axis Z position signal for depth control purposes. For this reason, three other depth sensors were installed in early 2015. These sensors are described in the next two sections.

1.7.2 Laser sensor

A Laser sensor is mounted 13.1° ahead of the tool (in the X-direction) and at the same vertical height (Y-direction) as the tool. It uses several beams to measure the distance to the copper, and averaging is used to derive the actual value. If the depth increases, the distance as measured by the Laser decreases, since the sensor is mounted on the Z-axis. The Laser signal is calibrated against the Axis Z position signal before the tool has touched the canister. The main drawbacks of the Laser sensor are that it:

- Partly captures the joint gap between the lid and the tube.
- Captures the difference in lid and tube diameter during the downward sequence, and throughout the joint line sequence.
- Sometimes has an increased magnitude in measurement noise (see Figure 1-9).

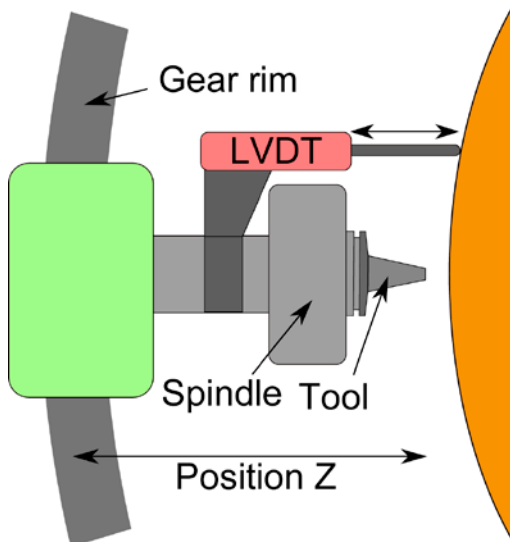


Figure 1-7. Overview of the depth sensor configuration used in SKB's welding machine. The Laser and LVDT sensors are located at the same position when seen from this angle.



Figure 1-8. Ball bearing tool.

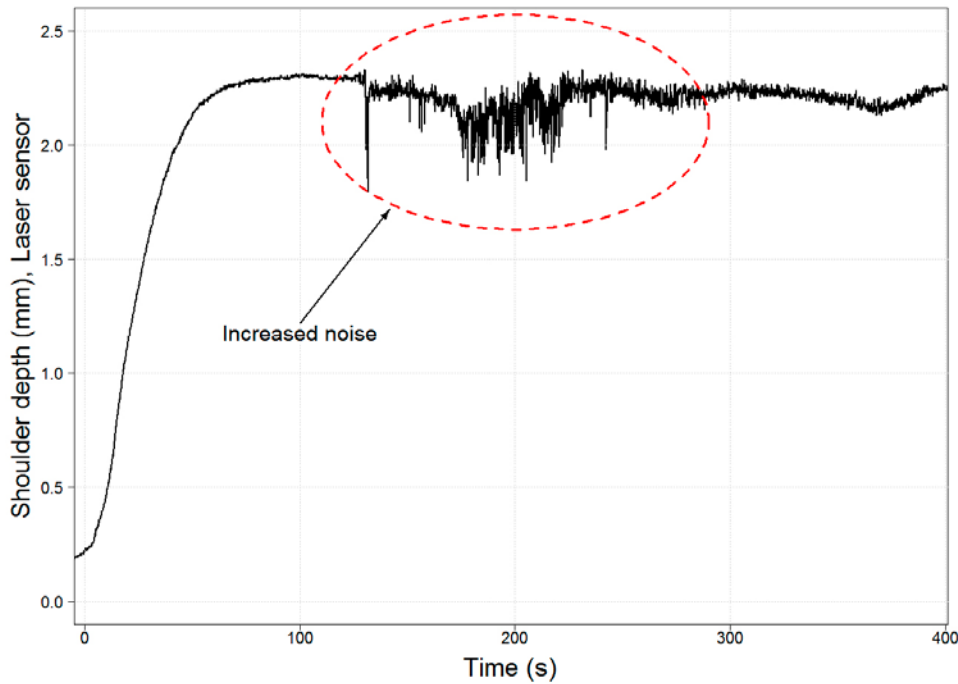


Figure 1-9. Temporarily increased measurement noise in the Laser sensor signal.

The cause of the increased amount of measurement noise has not yet been investigated. A guess is that the sensor might be sensitive to machine vibration.

Since the Laser is mounted on the Z-axis, it lacks several of the disadvantages of the Axis Z position sensor. However, it remains sensitive to the effect of thermal expansion at the tool, since it cannot be placed directly at the tool. This difference is currently not addressed, assuming repeatability between welds, and future work will show whether or not this is a valid assumption.

1.7.3 LVDT sensors

Two LVDT sensors (LVDT1 and LVDT2) are mounted 13.1° ahead of the tool (in the X-direction, see Figure 1-10). LVDT1 is positioned 32.5 mm above the tool centre (in the Y-direction), and LVDT2 is 32.5 mm below the tool centre. LVDT1 thus measures depth with respect to the lid during the entire weld. LVDT2, on the other hand, measures depth with respect to the tube during the joint line sequence and with respect to the lid during the remainder of the weld. Since the lid and the tube never have exactly the same diameter (due to different thermal boundary conditions resulting in different thermal expansions), the lid/tube transition will always be seen in the LVDT2 signal (see Figure 1-11). Taking the difference between the two LVDT sensor signals, it is thus possible to get a measure of the difference in diameter between the tube and the lid. Both LVDT-signals are calibrated against the Axis Z position signal before the tool has touched the canister.

If the LVDT sensors move towards the copper, they register a greater depth, and they report a smaller depth if they move away. If the tool goes deeper into the weld, they will register a greater depth. However, if the tool stands still and either LVDT moves over a bump, they will register a depth increase, since the distance to the copper decreases. By this logic, the transition shown in Figure 1-11 actually suggests that the tube has a larger outer diameter than the lid. The same holds for the u-shaped “depth decrease” just after the transition. This is the result of a pre-weld BBT measurement, which has left a thin trace in the tube surface.

Much like the Laser sensor, the two LVDT sensors lack several of the disadvantages of the Axis Z position sensor. They are, however, sensitive to the effect of thermal expansion on the tool position. This difference is currently not addressed, assuming repeatability between welds. LVDT1 has few to

no disadvantages apart from measuring the thermal expansion difference between its location and the location of the tool. It could, however, be problematic to use LVDT2 in the controller, because of the lid/tube transition.

1.7.4 Shoulder outer diameter temperature

All three temperature measurements depend mainly on the power input, but it can be shown that the temperature recorded by the sensor placed furthest out on the shoulder (Shoulder OD, see Figure 1-4) is also related to the depth. This is reasonable since the sensor is placed so far out that the shoulder is not necessarily in contact with the copper at this location. Therefore, the deeper the weld is, the greater this temperature will be. This indicator will also be used to model the depth.

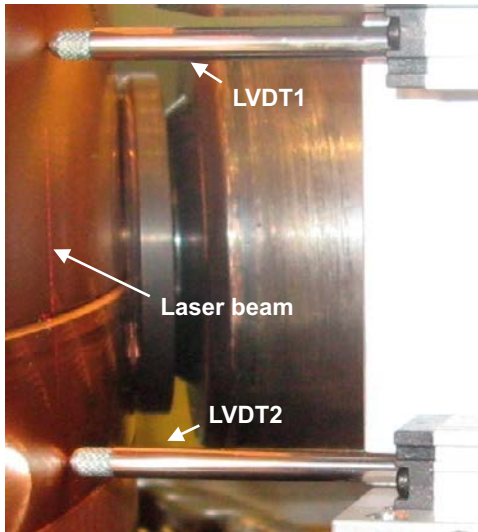


Figure 1-10. The two LVDT sensors and the red Laser beams during the joint line sequence. The tool is in the middle, 13.1° behind (in the x-direction).

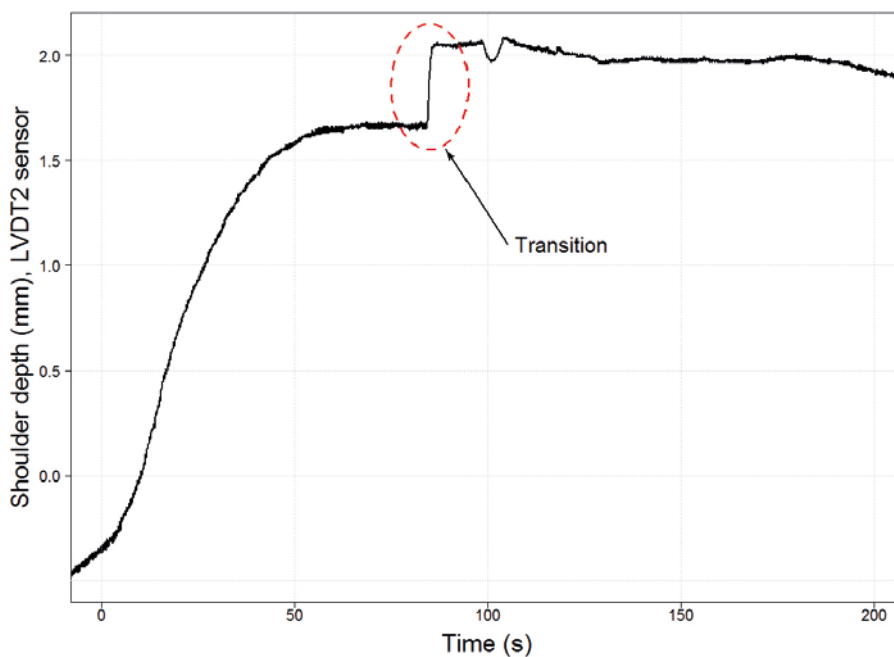


Figure 1-11. The LVDT2 transition from lid to tube is marked. This suggests that the tube is approximately 0.4 mm thicker than the lid.

1.8 Measures of the actual depth

It is difficult to measure the actual depth, even if the canister is cut up into macro samples like the ones in Section 5.2. The stirred zone, called the nugget, is larger than the probe, and its size also depends on the welding temperature (although this effect may be negligible since the welds are temperature controlled).

An easier way to estimate the depth is by measuring the shoulder footprint. The convex shoulder geometry is known, so it is possible to estimate the shoulder depth from measurements of the shoulder footprint width. The shoulder footprint depth, z_{sd} , can be calculated from the footprint width, FW , using the shoulder geometry. The maximum diameter of the shoulder is 70 mm, and the diameter of the probe is 30 mm at the base. Hence, the minimum footprint width (given that the shoulder touches the copper) is 30 mm, and the maximum width is 70 mm (when the full shoulder is in contact with the copper). The shoulder footprint depth (in mm) can then be calculated using the following equation

$$z_{sd}(FW) = \begin{cases} 0, & FW \leq 30 \text{ mm}, \\ 3, & FW \geq 70 \text{ mm}, \\ R \left(1 - \cos \left(\sin^{-1} \frac{FW + 2c - 2R_{probe}}{2R} \right) \right) - \rho, & 30 \text{ mm} < FW < 70 \text{ mm}. \end{cases} \quad (1-1)$$

$R = 100$ is the radius of the spherical curvature of the shoulder, $R_{probe} = 15$ is the radius of the probe at the base, $c = 4.758$ is an offset parameter for the centre of the spherical curvature, and $\rho = 0.1133$ is a parameter that compensates for material that has been milled off the shoulder. Note that this equation assumes that the lid and canister surfaces are aligned. In reality, the footprint is slightly asymmetric. Equation (1-1) provides the best estimation of the true shoulder depth currently available and will thus be used for comparison with the different sensors to evaluate their practical use as feedback signals in the depth controller.

The shoulder footprint widths from welds in the depth controller verification series have been measured by attaching a paper over the welds, and then sketching the contours of the shoulder footprint using a pencil. This method produces detailed sketches of the welds, and the footprint widths are measured using a dial caliper at every 1 cm. The first part of a sketch is seen in Figure 1-12. The shoulder footprint widths during the downward sequence have been measured perpendicular to the centre line. In chapter 6, the depth controller verification welds are compared to 18 welds without the depth controller activated. Several of these welds' footprints have been measured by a cruder method, using a ruler to measure the footprint directly. The shoulder footprints are measured at a point two degrees (18 mm) into the joint line sequence, where the footprint is more easily measured.

Another option, that may be considered in the future, is to add an optical instrument behind the tool that can measure the footprint during welding. Such measurement could also be used for feedback to the depth controller.

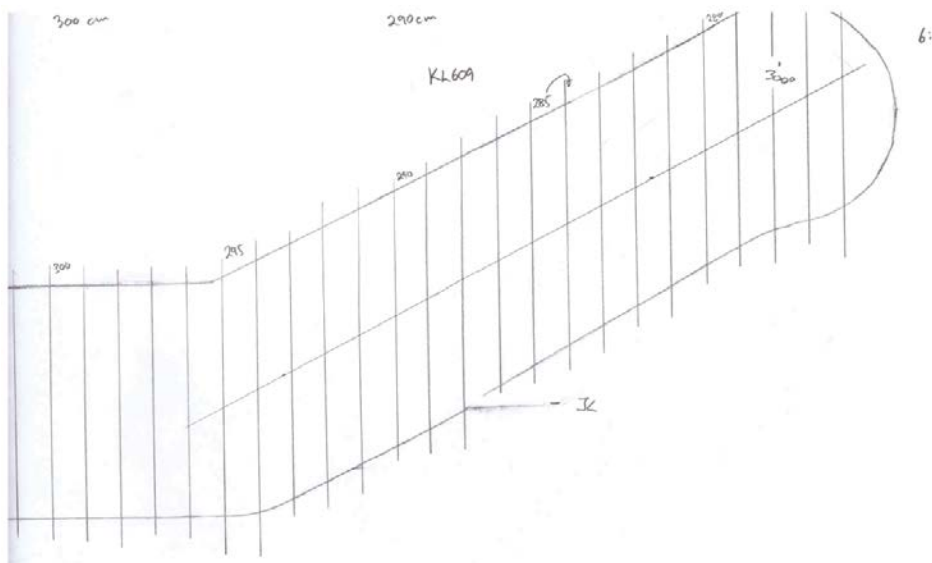


Figure 1-12. Sketch of the shoulder footprint. The footprint width during the downward sequence was measured perpendicular to the centre line.

2 Factors that influence depth

2.1 Hardness

Hardness is a measure of how difficult it is to penetrate a solid. The hardness of copper vary, for example due to different microstructure (like grain size) from different manufacturing techniques or heat treatments. Hardness has only been measured irregularly for the various copper lids and tubes. Pilot hole forming has, on the other hand, been performed almost identically for the last several hundred welds, using the same drill hole size and forming depth. Measuring the maximum Z-force needed to create this hole thus provides a consistent measure of the lid hardness (see Figure 2-1). There have been experiments with other drill hole sizes and forming depths, as well, but it was decided to keep these two parameters consistent for all welds, as they had a negligible effect on depth.

It is clear that lid hardness will have an effect on depth, as it is more likely that soft lids/rings result in deep welds than do harder lids/rings. Figure 2-2 shows how well lid hardness correlates with shoulder depth at the point where the start sequence begins. At the joint line, it seems reasonable to believe that a combination of lid and tube hardness determine the total effect of hardness on depth, but so far there have been no consistent measures of tube (ring) hardness.

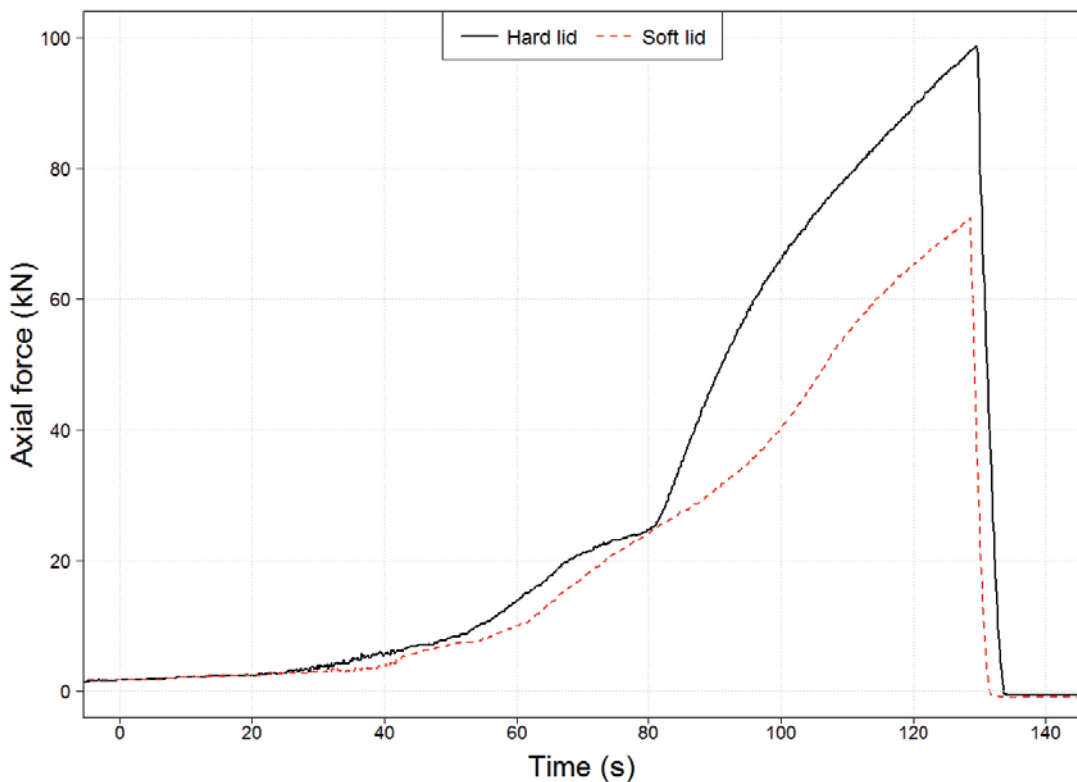


Figure 2-1. The maximum axial force during pilot hole forming gives a measure of copper hardness. The harder the lid is, the greater the axial force needs to be to reach the same depth.

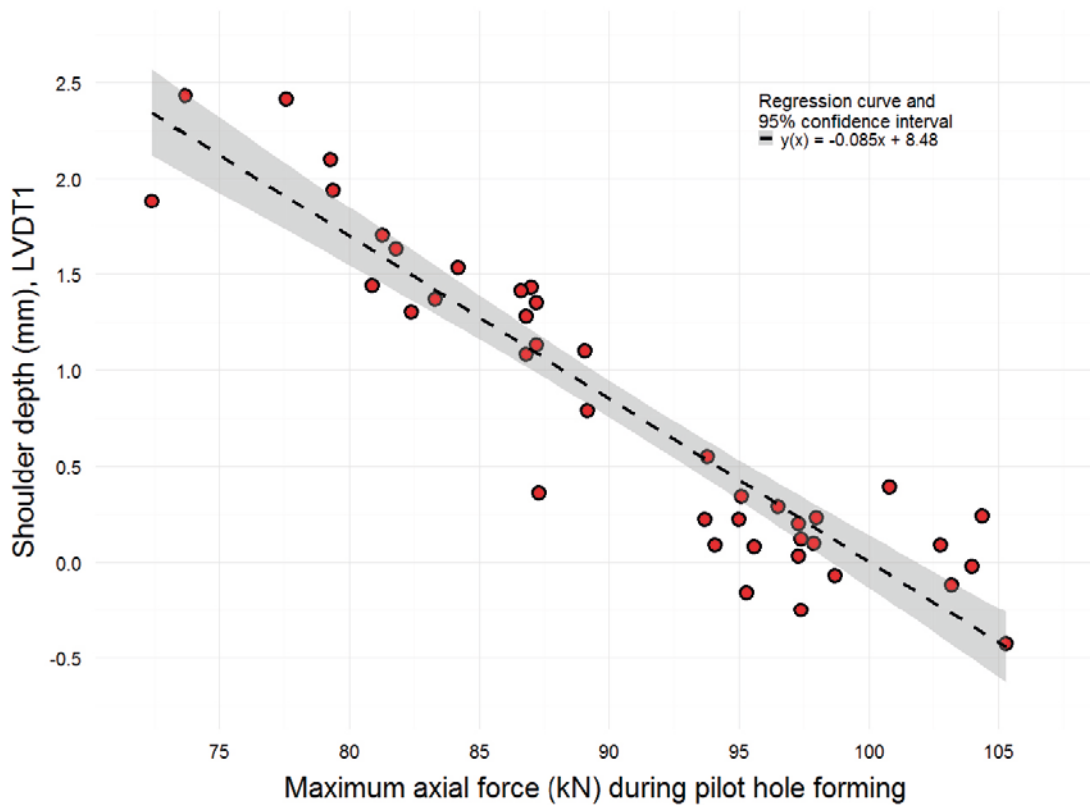


Figure 2-2. The shoulder depth when the start sequence begins is highly dependent on the lid hardness, here measured by the maximum axial force during pilot hole forming. A one variable regression curve is plotted with a dashed black line, together with its 95 % confidence interval in grey.

2.2 Heat-up time, total power input, and transition temperatures

Here, heat-up time refers to either the total time spent in a certain sequence (dwell or start), or the time spent in dwell until a specific temperature is reached (a probe temperature of 750 °C is used here). The start and downward sequences both begin at predefined probe temperatures (see Figure 2-3). The heat-up time is also strongly related to the power input during the specified time interval. Figure 2-4 shows how the heat-up time to a probe temperature of 750 °C is related to average power input during the same time interval.

A weld with a longer dwell or start sequence will typically be deeper (see Figure 2-5). This is intuitive, since a longer dwell or start sequence gives the tool more time to dig into the copper (since constant axial force is used).

Table 2-1. Weld comparison with and without power control during the dwell sequence.

	Power control	No power control
Total number of welds investigated	58	130
Average mean power to a probe temperature of 750 °C	34.8 kW	32.1 kW
Max difference in mean power to probe temp 750 °C	2.6 kW	12.1 kW
Standard deviation in mean power to probe temp 750 °C	0.5 kW	2.1 kW
Average heat-up time to probe temp 750 °C	231 s	319 s
Max difference in heat-up time to probe temp 750 °C	155 s	515 s
Standard deviation in heat-up time to probe temp 750 °C	30 s	84 s

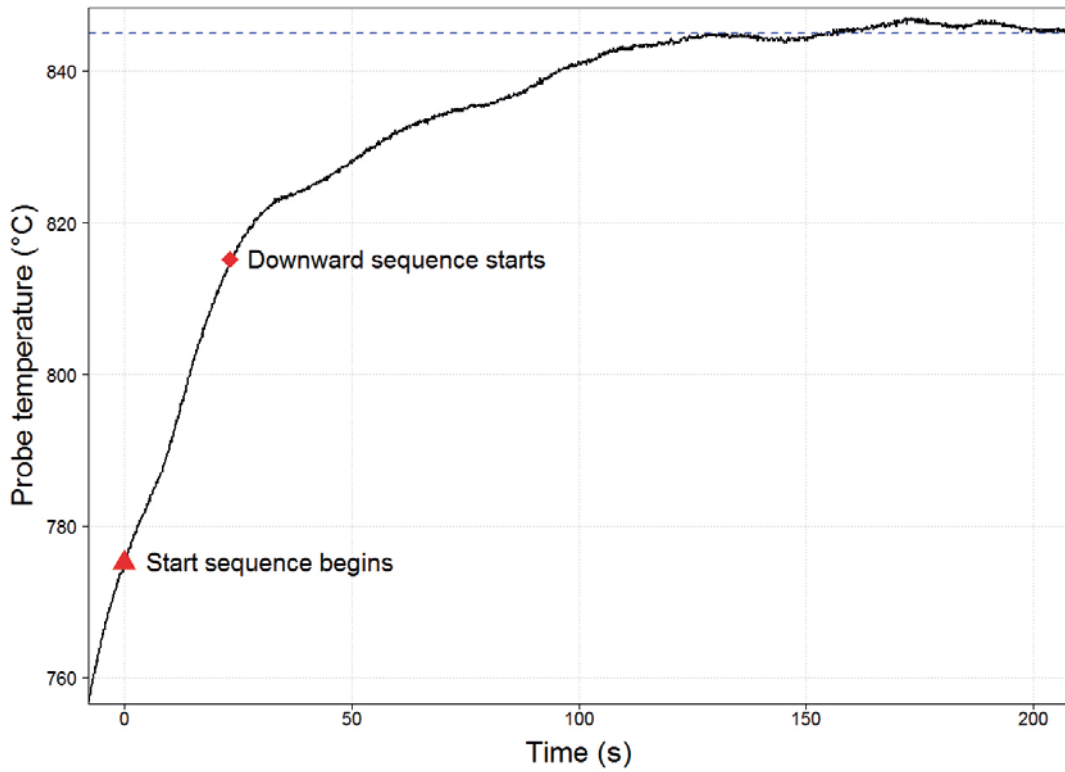


Figure 2-3. The start and downward sequences begin at pre-specified probe temperatures, usually 775 °C and 815 °C, respectively. The dashed blue line shows the probe temperature reference.

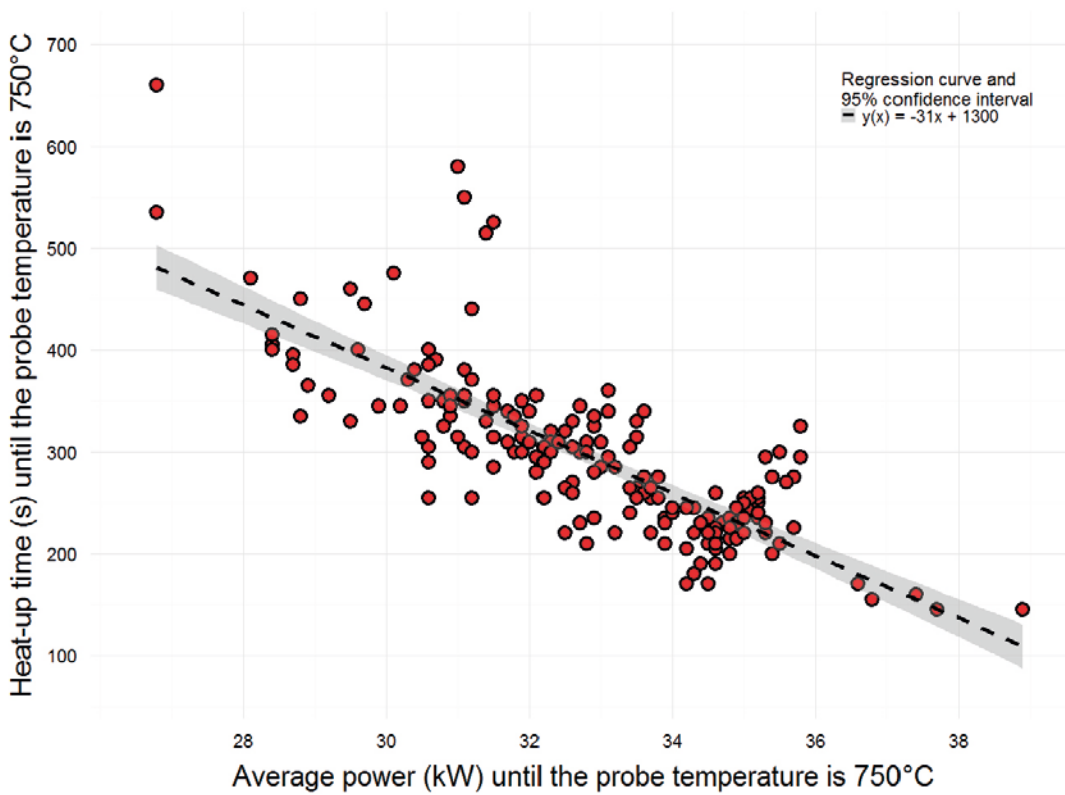


Figure 2-4. The relationship between the average power input and heat-up time from the start of the dwell sequence until the probe temperature is 750 °C (also dwell). A one variable regression curve is plotted with a dashed black line, with its 95 % confidence interval in grey.

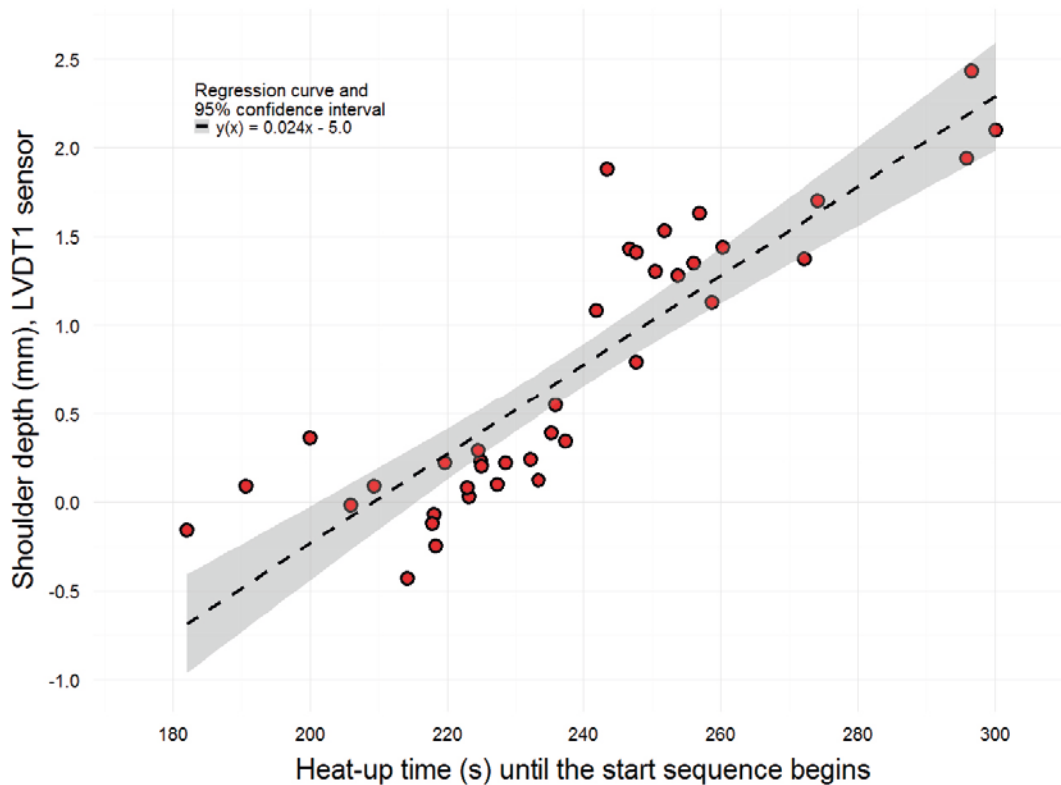


Figure 2-5. The relationship between heat-up time and LVDT1 shoulder depth when the start sequence begins. One variable regression curve is shown as a black dashed line, with its 95 % confidence interval in grey.

In an attempt to decrease the impact that a long heat-up time has on depth, power control has been added to the dwell sequence (Cederqvist 2011). The power is thus forced to increase at a certain rate during the entire dwell sequence. This has, in turn, led to much less variation in the heat-up times and to shallower welds in soft lids. Table 2-1 summarizes statistics from welds before and after the power control was included in the dwell sequence. It shows that the variation in average power and heat-up time have decreased dramatically after this change.

2.3 Axial force

The higher the axial force, the deeper the weld will be. This effect has previously been modelled in Nielsen et al. (2013), and the axial force is currently the only parameter manipulated by the depth controller. The depth controller actually chooses an axial force reference, which is in turn fed to a force controller. The reference has minimum and maximum limits (82 and 89 kN, respectively, in the verification welds). The lower limit is chosen to decrease the risk of wormhole defects (Cederqvist et al. 2012b), and the upper limit is chosen based on experimental evidence that shows no weld (out of more than 600) has ever needed a higher axial force to avoid defects.

3 The depth controller

3.1 Automatic control

Automatic control is a science that utilizes measurement signal feedback. Examples of automatic control are cruise control in cars and temperature control in a house. In cruise control, the measured current vehicle speed is compared to the desired speed (usually called the reference signal) that the driver has set. A controller uses the difference between these two signals, called the control error, to choose the magnitude of a control signal that can manipulate the speed. In this case, the throttle is used as the control signal.

Automatic control is typically used in processes with behaviour that is difficult to predict or processes that are too safety critical to control manually. Both these conditions hold for SKB's welding process, where both the temperature and depth need to be controlled simultaneously. Changing the axial force also affects the temperature, since the torque increases with increased force. Even if the depth controller is turned off, temperature control is still challenging, considering its varying thermal boundary conditions and rapid torque disturbances.

3.2 The PID controller

The Proportional-Integral-Derivative (PID) controller is by far the most commonly used controller in industry. A PID controller is divided into three different parts, each with a different treatment of the control error that contributes to the final control signal: a proportional part that reacts to the current control error, an integral part that summarizes the control error over time, and a derivative part that predicts future control errors. This paradigm comprises one part reflecting the present, one the past, and one the future. This intuitive explanation is an important factor in the popularity of the PID controller.

The power, temperature, and depth regulators of the SKB welding process are all PID controllers, parameterized according to the continuous-time formula

$$u(t) = Ke(t) + \frac{K}{T_i} \int_0^t e(\tau) d\tau - KT_d \frac{de(t)}{dt} \quad (3-1)$$

Here, u is the control signal calculated by the PID algorithm and e is the control error (for example, the difference between the desired depth and the actual depth). Both variables depend on time t . K denotes the proportional gain, T_i the integral time, and T_d the derivative time. These PID parameters are all set before the controller is activated, and they determine the speed, stability margins, and noise sensitivity of the controlled process.

The actual PID algorithm implemented on the FSW process includes some other features that are necessary for the control to run smoothly. These include set-point weighting on the P- and D-parts, measurement noise filtering, and anti-windup tracking (see for example Åström and Hägglund (2006) for an explanation of these terms). The depth controller also uses a third-order reference filter that makes the control signal less active when it is first enabled at the beginning of the start sequence.

3.3 Depth controller

The depth controller implemented on the FSW machine uses the axial force reference as its control signal. The minimum and maximum limits of this reference are set to 82 and 89 kN, respectively, during the verification welds. A PI controller (that is, a PID with derivative time set to zero) is used in the same welds, with parameters $K = 3.28$ and $T_i = 2.25$.

Investigating simulations of the controlled process, it has been concluded that the performance improvement provided by a PID controller (rather than a PI) does not justify the added complexity of such a controller. Hence, a PI controller is used to regulate the depth. The tuning of the PI controller is performed using the model-based optimization approach presented in Garpinger and Hägglund (2008). This tuning method selects the best-performing PI controller (in terms of minimizing the integrated absolute control error) while keeping stability within user-defined margins. The controller used currently is tuned to have large stability margins rather than high performance. However, it can be retuned in a future version of the controller, if necessary. The reference filter used is described by the following transfer function:

$$F_r(s) = \frac{1}{(1 + 15s + 56.25s^2)(1 + 7.5s)} \quad (3-2)$$

The parameters in the third-order filter above have been chosen such that the depth reference mimics the increase in depth for a weld with constant axial force. The motivation for this approach is to prevent the axial force from varying drastically during the beginning of the downward sequence. The choice of parameters is not yet final, and more investigations are needed to determine the best reference filter for this application.

The depth controller can use any of the LVDT1, LVDT2, Laser, or Axis Z position sensors for depth measurement feedback. During the verification welds, the Laser sensor has been used. However, one of the purposes of this study is to decide which sensor is best suited for the task. The result might also be that a combination of the sensor signals is preferred.

At present, the depth controller is only active during the start and downward sequences and the first 20 seconds of the joint line sequence. It is assumed that the depth remains fairly constant during the joint line sequence and that the start and downward sequences are the most important in setting the depth of the full weld. The objective of the depth controller is therefore to achieve the desired shoulder depth at the point where the joint line is reached. Hence, tracking the desired shoulder depth during the initial part of the downward sequence is not as high a priority as is reaching the desired depth at the joint line.

If future studies show that it is necessary to control the depth throughout the joint line sequence or during the overlap sequence, then the control will be extended accordingly. Before such changes are made, it is important to first investigate both how well the depth sensors capture the actual depth, and if defect are formed during the joint line and/or overlap sequence.

4 Questions for the report to answer

One of the objectives of this report is to provide answers to the following questions:

1. Which sensors can be used to estimate the depth? How accurately can the depth be estimated?

Since the shoulder footprint depth is currently the best measure of the actual depth, it is used to evaluate the various depth sensors and indicators. To simplify statistical analysis, data from the verification welds is complemented with results from welds without active depth control. These data is also used to answer several of the other questions presented in this section.

2. Which sensor signal(s) should be fed back to the controller?

Currently, the controller can use any of the four depth sensors (Axis Z position, Laser, LVDT1, LVDT2) as its feedback signal. Are any of these sensors best suited for the task, or should a different signal altogether be used? Might a linear combination of the sensors be the best choice?

3. What shoulder depth reference should be used?

The verification welds use a reference of 2.2 mm for the depth, measured by the Laser sensor. Do the macro samples show any signs of joint line hooking or joint line remnants? Is there any flash formation during the welds? If it is decided to use a feedback sensor other than the Laser signal, what reference value should then be used?

4. Is it possible to control the depth with sufficient accuracy? What limitations are there?

Do the axial force saturation limits or the material hardness constrain the achievable depth? What does the report on the macro samples reveal?

5. What alternative strategies might be used to control the depth?

Currently the depth controller is only active during the start and downward sequences and the first 20 seconds of the joint line sequence. Is there already a need for depth control during the dwell sequence? If so, how should it be carried out?

6. How can a fail-safe depth control strategy be implemented?

Can a fail-safe control strategy that changes based on which sensors are still functioning, that is, similar to the safety system already implemented for the temperature control, be implemented?

5 Depth controller verification welds

Thirteen welds have been carried out to analyse and evaluate the performance of the depth controller. Twelve welds (with ID's 604–615) are short (60°) and made in two different lids (TX-178, TX-186, from SKB) and rings (both from tube T76), while the one full circumferential weld (ID 640) has been made in a single lid (PLF-7, from Posiva Oy) and ring (from tube T85). Furthermore, there are two reports on the macro samples, one from welds 604–615 (Hjertsén 2016a) and one from weld 640 (Hjertsén 2016b). Additionally, since weld 640 is a full weld, it is not possible to measure the shoulder footprint 2° into the joint line sequence (due to the overlap).

Four previously unused tools (MT221–224) and shoulders (MC90, MC103, MC118, MC120) have been used for three short welds each. The tool (MT261) and shoulder (MC114) used for the full weld were also previously unused. The hardness of each lid has been measured at each weld start position, using the maximum axial force during pilot hole forming, see Table 5-1.

Each lid is marked with a different colour. The first lid has an average hardness of 97.5 kN and is thus slightly harder than the second lid, which has a mean hardness of 95.3 kN. These two lids are much harder than the last lid, which has a hardness of 72.4 kN at the weld start point. Earlier hardness measurements have shown Posiva lids to be generally softer than SKB lids (due to different manufacturing techniques and heat treatments).

As already stated, the Laser sensor is used as the feedback signal in the depth controller, and the shoulder depth reference is 2.2 mm. The axial force reference has an upper saturation limit of 89 kN and a lower limit of 82 kN.

Table 5-1. Lid hardness, measured by maximum axial force (kN) forming the pilot hole.

Weld ID	604	605	606	607	608	609	610	611	612	613	614	615	640
Hardness	98.0	97.3	95.6	97.4	97.9	98.7	93.7	95.1	97.4	95.0	96.5	93.8	72.4

5.1 Results from the verification welds

Weld data from welds 604–615 and 640 (2° into the joint line sequence) are collected in Table 5-2, together with mean values, max deviation, and standard deviation. The difference between LVDT1 and LVDT2 (Diff LVDT) and the Shoulder OD temperature are provided along with the depth sensor measurements. LVDT1 data from weld 614 has been rejected because of a sensor failure. It is still unclear what caused this error.

Figures 5-1 to 5-4 show how the depth sensor measurements vary for the first 400 seconds of the thirteen verification welds (counted from the beginning of the start sequence). The starts of the joint line sequences are marked by black squares in the figures. The data has been smoothed in Matlab using smoothing splines with different choices for the smoothing parameter. These parameters have been given low values (which gives a larger smoothing effect) for signals with high measurement noise (Laser) or abrupt changes (LVDT2 and Axis Z position), and high values for already smooth signals (LVDT1). The purpose of the smoothing is to make the plots less cluttered. Figure 5-5 shows the control signals from each weld, that is, the axial force reference during the first 400 seconds of the thirteen welds.

Figure 5-1 shows the thirteen Laser measurement signals and their relative positions with respect to the reference value (dashed black line). At a point 2° into the joint line sequence, the Laser signal values are larger than the reference value for almost all of the welds, and the largest control error is 0.20 mm. The fact that so many welds seem relatively unaffected by the controller (the depth remains almost constant) suggests that it is a difficult process to control. A look at the control signals in Figure 5-5 reveals that many of the welds eventually exhibit a saturated axial force, thus constraining what the controller can possibly achieve. It remains to be seen if this gives sufficient accuracy.

Figures 5-2 and 5-3 show complementary measurement signals for LVDT1 and LVDT2. At a point 2° into the joint line sequence, LVDT1 varies slightly more than Laser (0.26 mm compared to 0.21 mm), while LVDT2 varies significantly more (0.60 mm). This variation is most likely because the LVDT2 value depends on the relative thickness of the lid and the tube. Generally, the LVDT1 signal is the smoothest of the four sensor signals (even before the smoothing splines are applied). For example, LVDT1 does not suffer from the kind of noise that can be present in the Laser signal (see Figure 1-9).

Figure 5-4 shows the Axis Z position signals, which vary widely, even though both static and force induced gear rim deflection have been compensated for. This sensor is obviously unsuitable for use in the depth controller.

Table 5-2. Data from depth controller verification welds, 2° into the joint line sequence. Diff LVDT is the difference between LVDT1 and LVDT2, Sho temp stands for Shoulder OD temperature (see Figure 1-4), and Fp is an abbreviation for footprint. Means, maximum deviation, and standard deviation are presented in the bottom rows.

Weld ID	Fp width	Fp depth	Laser	LVDT1	LVDT2	Diff LVDT	Sho temp
604	67.8	2.73	2.39	2.24	2.43	-0.19	719.5
605	68.9	2.86	2.23	2.07	2.21	-0.14	717.5
606	68.1	2.76	2.23	2.05	2.23	-0.18	716.5
607	67.1	2.64	2.30	2.11	2.20	-0.09	710.0
608	66.1	2.52	2.23	2.14	2.37	-0.23	707.5
609	67.4	2.68	2.24	2.01	2.12	-0.11	707.5
610	67.6	2.70	2.36	2.17	2.64	-0.47	718.5
611	67.4	2.68	2.40	2.22	2.54	-0.32	725.5
612	67.1	2.64	2.37	2.21	2.34	-0.13	724.0
613	66.9	2.62	2.36	2.27	2.23	0.04	687.5
614	66.5	2.57	2.22	-	2.04	-	689.0
615	66.5	2.57	2.21	2.04	2.23	-0.19	684.0
640	-	-	2.19	2.05	2.19	-0.14	722.7
Mean:	67.3	2.66	2.29	2.13	2.29	-0.18	710.0
Max dev:	2.8	0.34	0.21	0.26	0.60	0.51	41.5
St. dev:	0.74	0.09	0.08	0.09	0.17	0.13	14.4

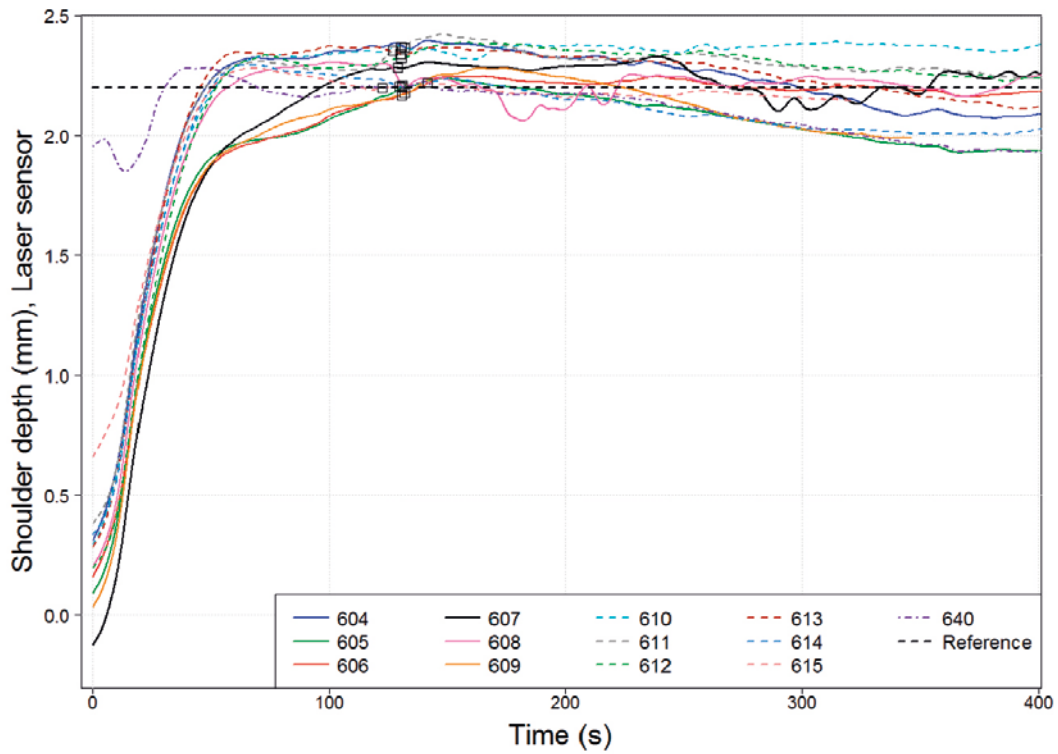


Figure 5-1. Laser sensor depth measurements during the thirteen verification welds. The reference depth is shown as a dashed black line. The starts of the joint line sequences are marked with black squares in the plot. The signals have been smoothed in Matlab using a smoothing parameter of 0.01.

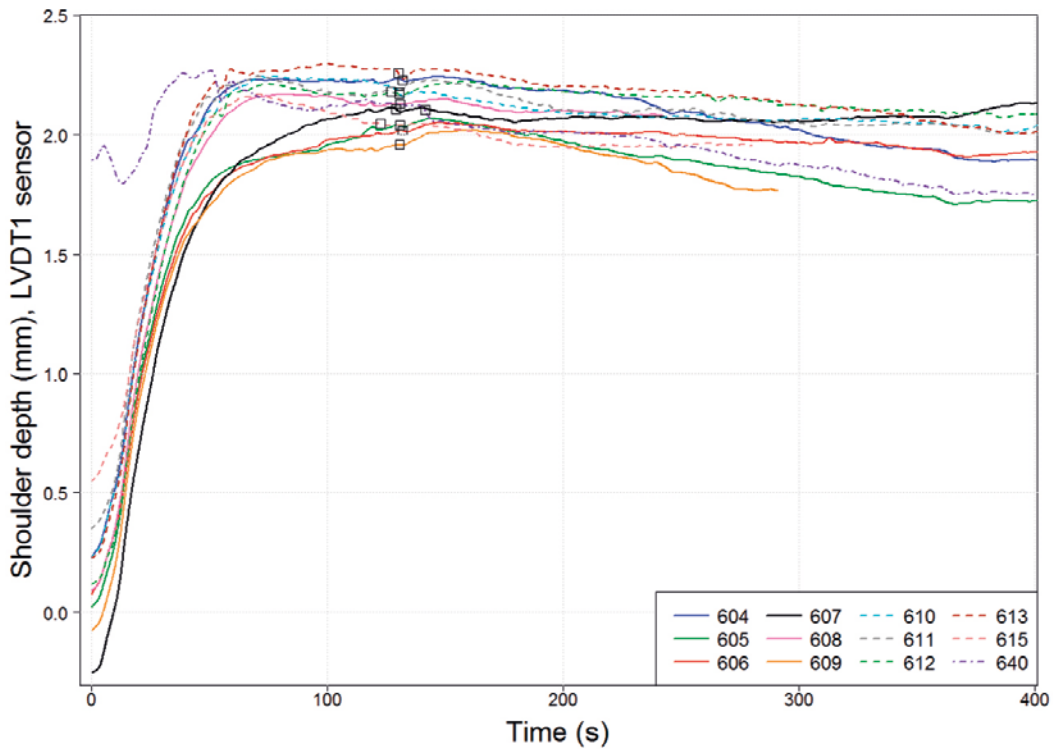


Figure 5-2. LVDT1 sensor depth measurements during twelve of the thirteen verification welds. The starts of the joint line sequences are marked with black squares in the plot. The signals have been smoothed in Matlab using a smoothing parameter of 0.2.

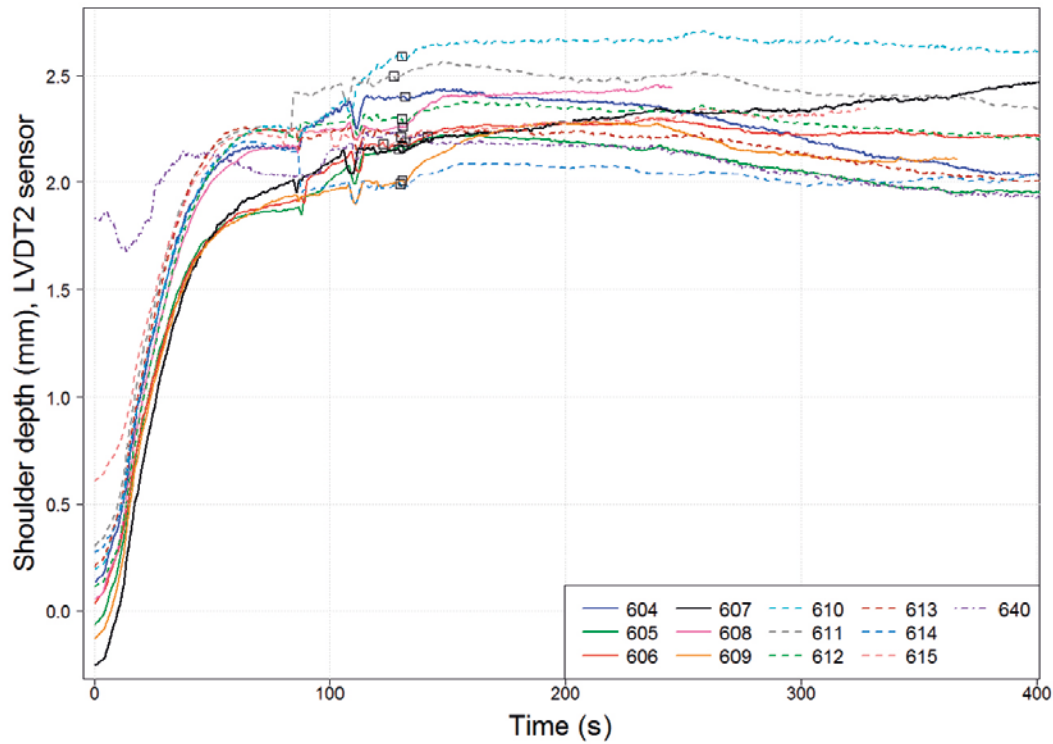


Figure 5-3. LVDT2 sensor depth measurements during the thirteen verification welds. The starts of the joint line sequences are marked with black squares in the plot. The signals have been smoothed in Matlab using a smoothing parameter of 0.95.

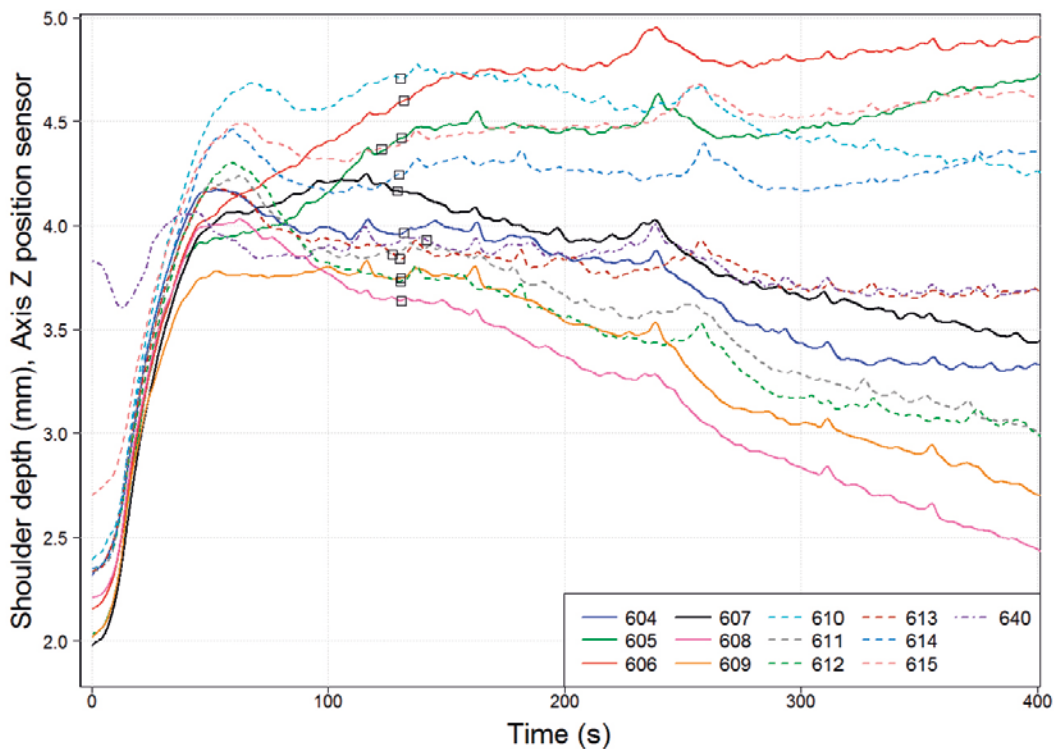


Figure 5-4. Axis Z position depth measurements during the thirteen verification welds. The starts of the joint line sequences are marked with black squares in the plot. The signals have been smoothed in Matlab using a smoothing parameter of 0.2.

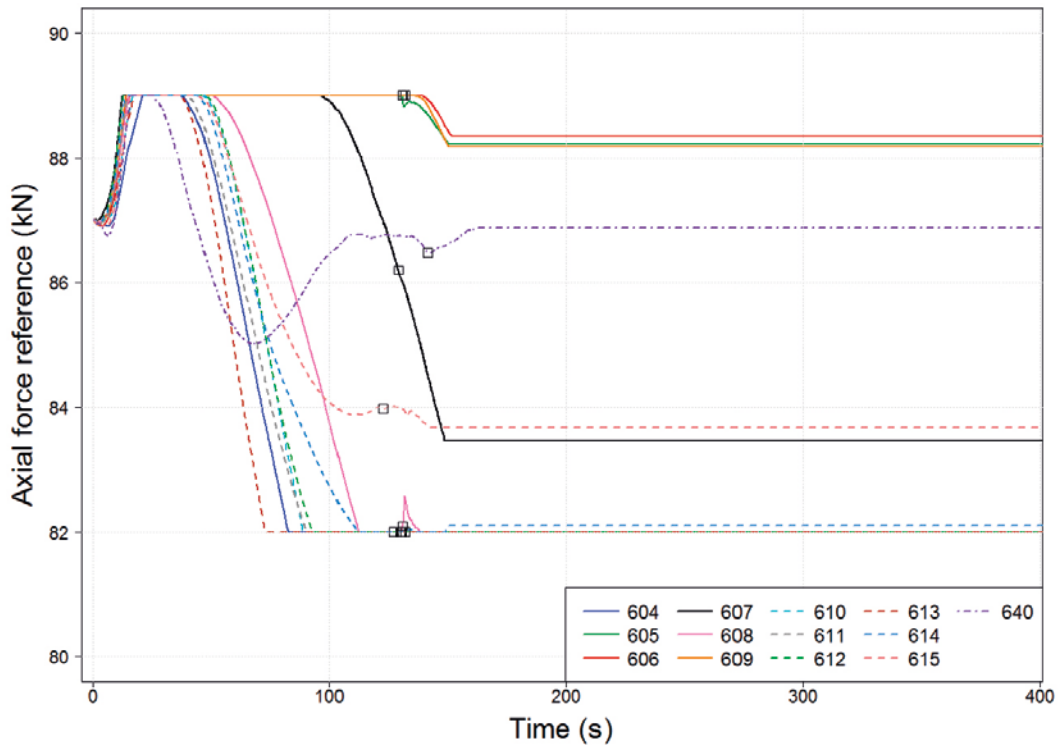


Figure 5-5. Axial force reference during the thirteen verification welds. No smoothing has been applied to the signals. The starts of the joint line sequences are marked with black squares in the plot. The controller remains active for 20 seconds after the joint line is reached.

The rest of the results presented in this section involve analysis of the shoulder footprint width in some way, and since it could not be measured for weld 640, this weld has been excluded from the remainder of this section.

Figure 5-6 presents the shoulder depth 2° into the joint line sequence as measured by the four depth sensors. Shoulder depths calculated from the shoulder footprint width (see Equation (1-1)) are also plotted. The dashed black line marks the reference depth that the controller tries to maintain. Only Laser depths should be directly compared to the reference value.

In Figure 5-7, the differences between the shoulder depth (estimated from shoulder footprint width) and the four sensor measurements are presented. The dash-dotted lines indicate the mean values of the differences. The means of the LVDT2 and Laser measurements are very similar and can be difficult to distinguish. Given that the shoulder footprint is a representative measure of the true shoulder depth, this plot gives estimations of the sensor errors 2° into the joint line sequence.

When the shoulder footprint widths are measured, the flash formations at the beginning of the joint line sequences are also measured. The results for the welds are presented in Table 5-3, revealing that all welds have no or very minor flash formations (0–1 mm). Welds 605–606 and 611 have flash formation, and from Figure 5-8, it can be seen that the tubes are significantly thicker than the lids. However, welds 604, 607 and 608, which have similar differences between the lid and ring, do not have any flash formation. The shoulder depths of welds 605–606 are slightly larger than those of welds 604 and 607–608, which, combined with the large difference between lid and ring, might have given rise to the flash formation. Weld 611 is not deeper than these welds, but the difference between lid and canister is significantly larger. The welds with less difference between lid and canister do not have any flash formation, either. This might indicate that a thicker canister (compared to the lid) gives flash formation when the shoulder depth is large enough, but more data is needed to validate this.

Table 5-3. Flash formation (in mm) during the beginning of the joint line sequence.

Weld ID	604	605	606	607	608	609	610	611	612	613	614	615
Flash	0	1	1	0	0	0	0	1	0	0	0	0

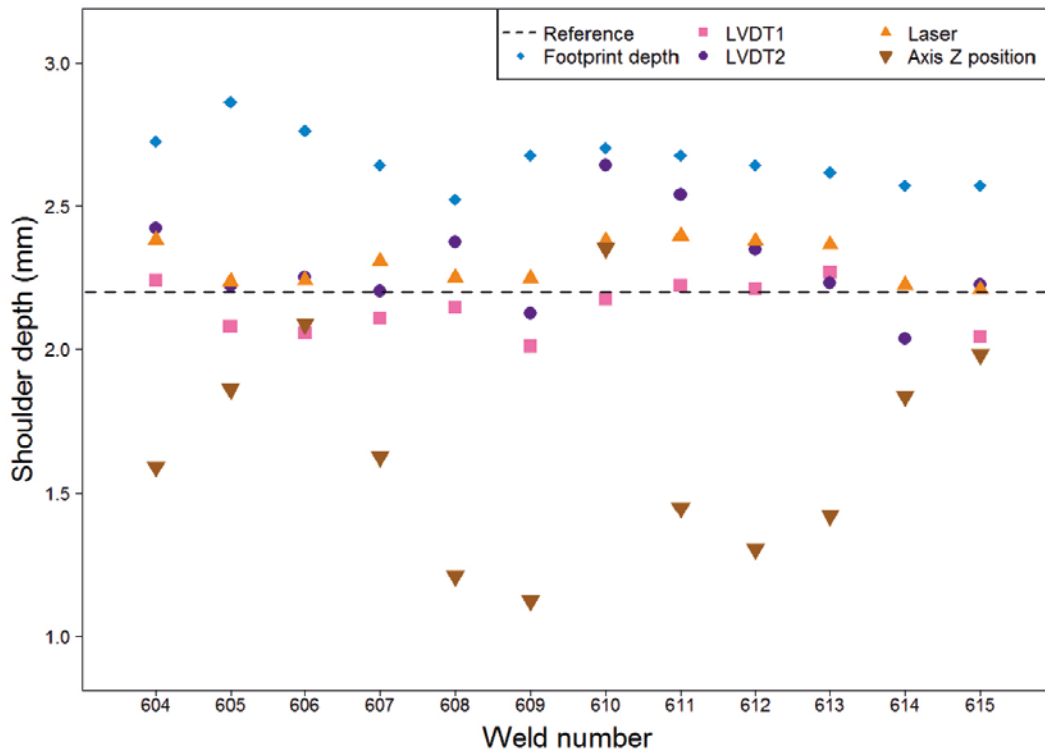


Figure 5-6. Footprint depth measurements 2° into the joint line sequence for welds 604–615 and corresponding shoulder depth measurements from the four different sensors. The controller reference value is indicated with a dashed black line.

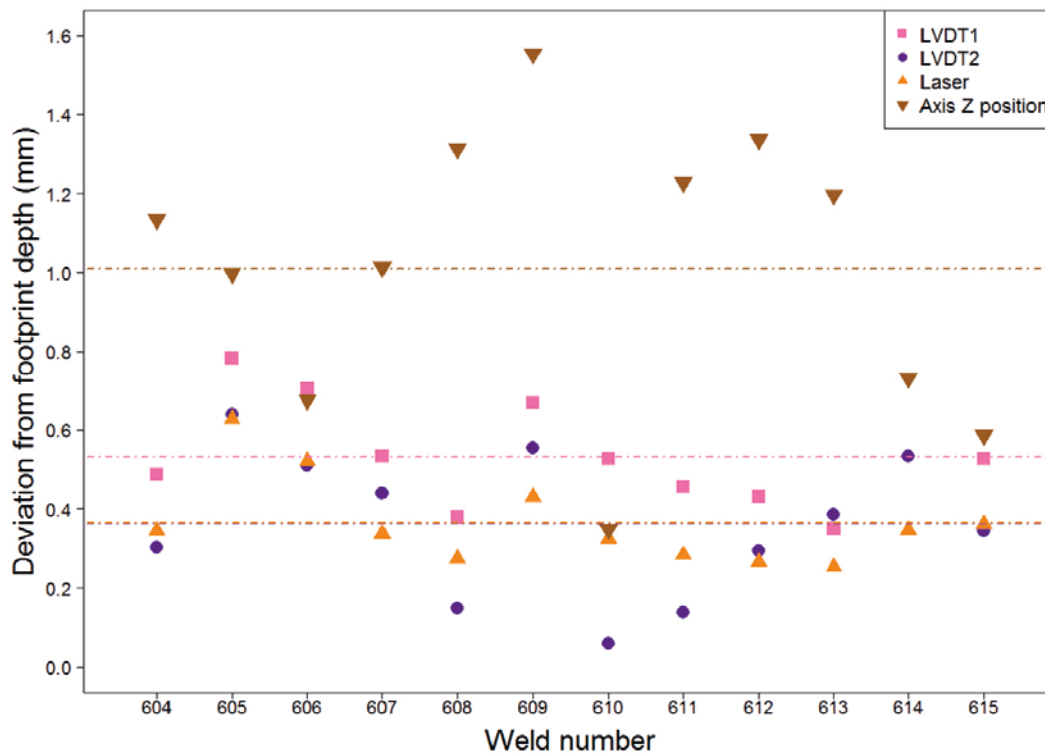


Figure 5-7. Differences between the footprint depth measurements 2° into the joint line sequence, and the corresponding shoulder depth measurements from the four different sensors for welds 604–615. Mean values of the differences are plotted as dash-dotted lines.

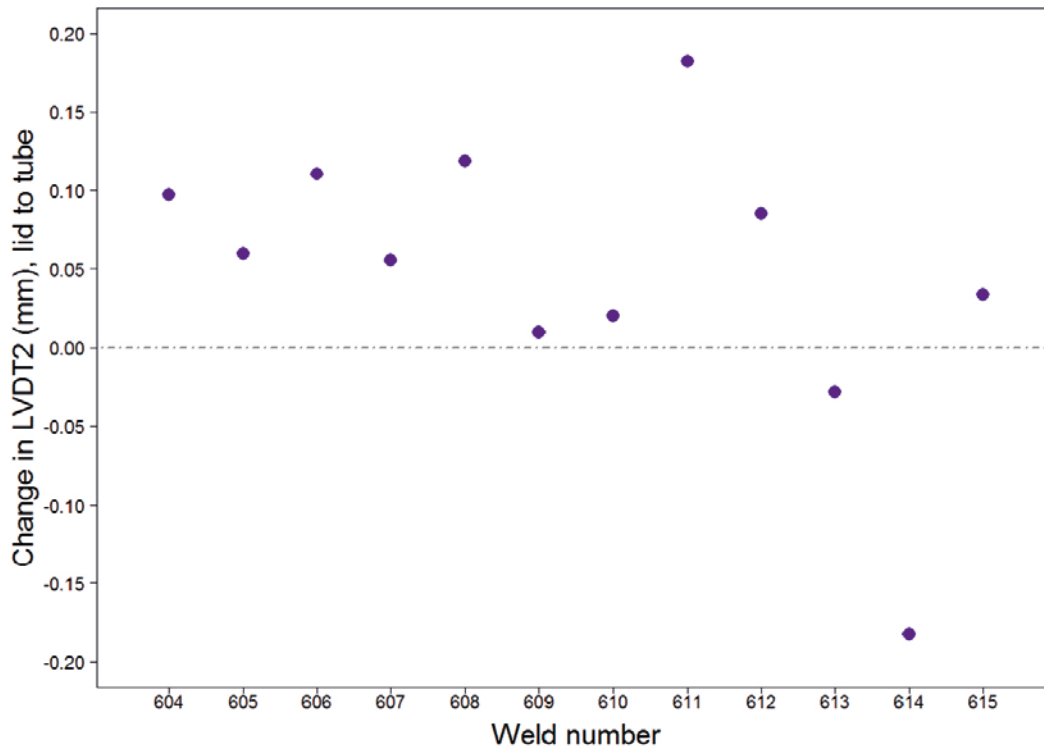


Figure 5-8. The difference in LVDT2 measurements just after and just before LVDT2 has entered the tube during the downward sequence. A positive value indicates a tube that is thicker than the lid.

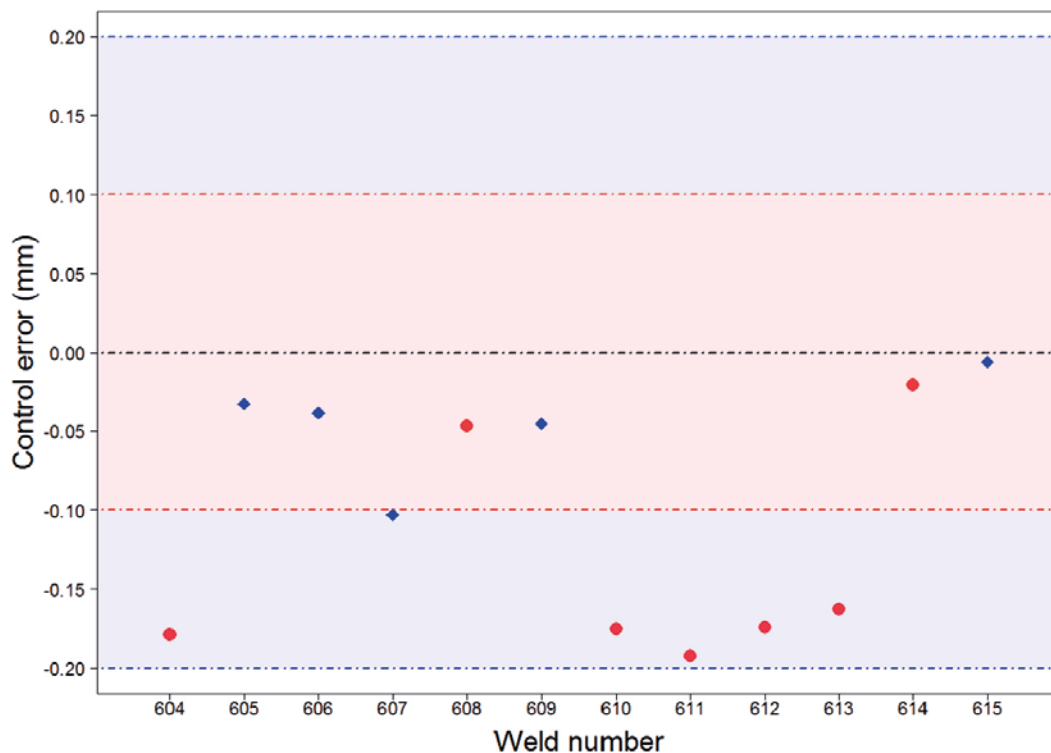


Figure 5-9. Control errors for each weld, 2° into the joint line sequence. The red and blue dash-dotted lines, together with the red and blue areas, represent control errors within ± 0.1 and ± 0.2 mm, respectively. The red circles represent welds limited at minimum force, and the blue diamonds represent welds with an unsaturated control signal.

The control errors 2° into the joint line are presented in Figure 5-9, where the welds marked with a red circle were saturated at the minimum force limit, while welds marked with a blue diamond had an unsaturated force at the same point. Six of the welds are within ± 0.1 mm, and six welds are within ± 0.2 mm. Furthermore, seven welds are saturated at the minimum limit force, and five welds are unsaturated (weld 608 is nearly at minimum force, though).

5.2 Results from the macro sample tests

Two macro samples have been collected from each of welds 604–615 (one based on the location with highest magnitude in the non-destructive testing (NDT) report and one random), and 18 samples from the full weld, 640 (9 based on the NDT and 9 random). No visible joint line hooking or horizontal joint line remnants are reported (Hjertsén 2016a, b).

A few of the macro samples are presented in Figures 5-10 to 5-12. Notice how the lid used for welds 604–609 has a much smaller grain size than the lid used for welds 610–615. Rather than joint line hooking, the vertical joint line has been pressed inwards (0.2–1.1 mm) in all welds, and Figure 5-13 reports the extent of this depression in each lid. It is reasonable to believe that welds with larger depressions are closer to producing joint line hooking than those with smaller depressions.

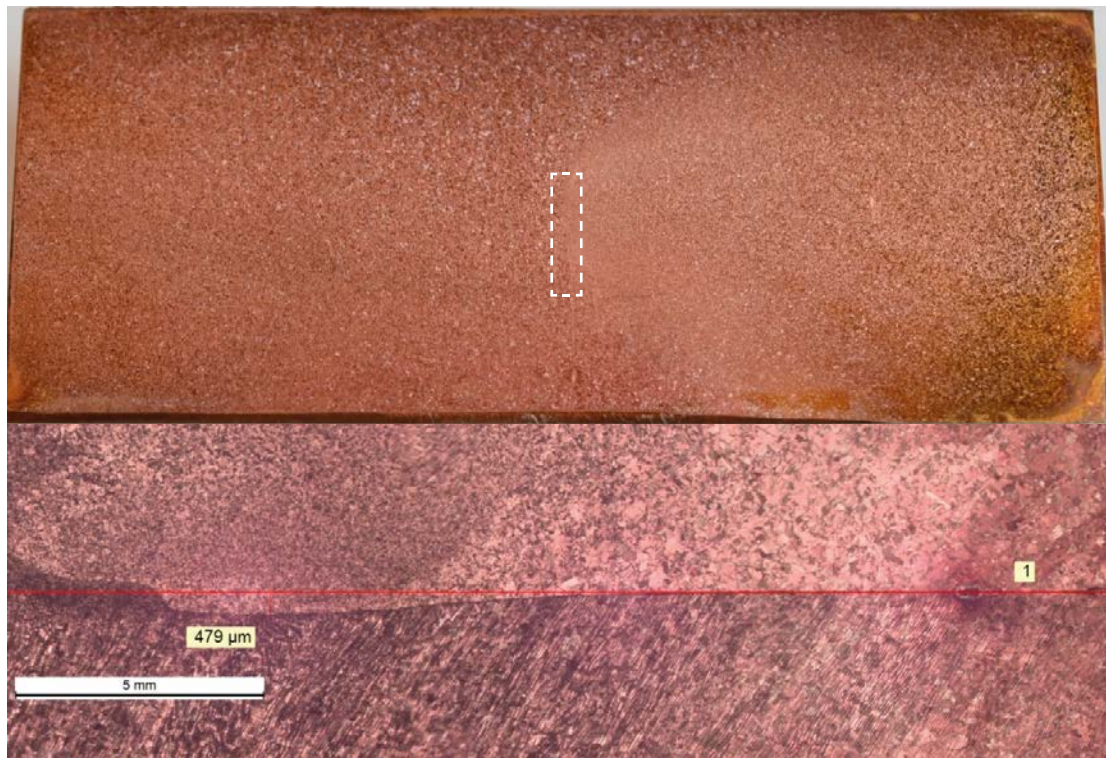


Figure 5-10. Macro sample from weld 604. The top picture shows the weld zone on the right hand side, while the bottom picture shows a zoom of the white dashed box (rotated 90° counter clockwise). A maximum depression of the vertical joint line of 0.479 mm was measured.

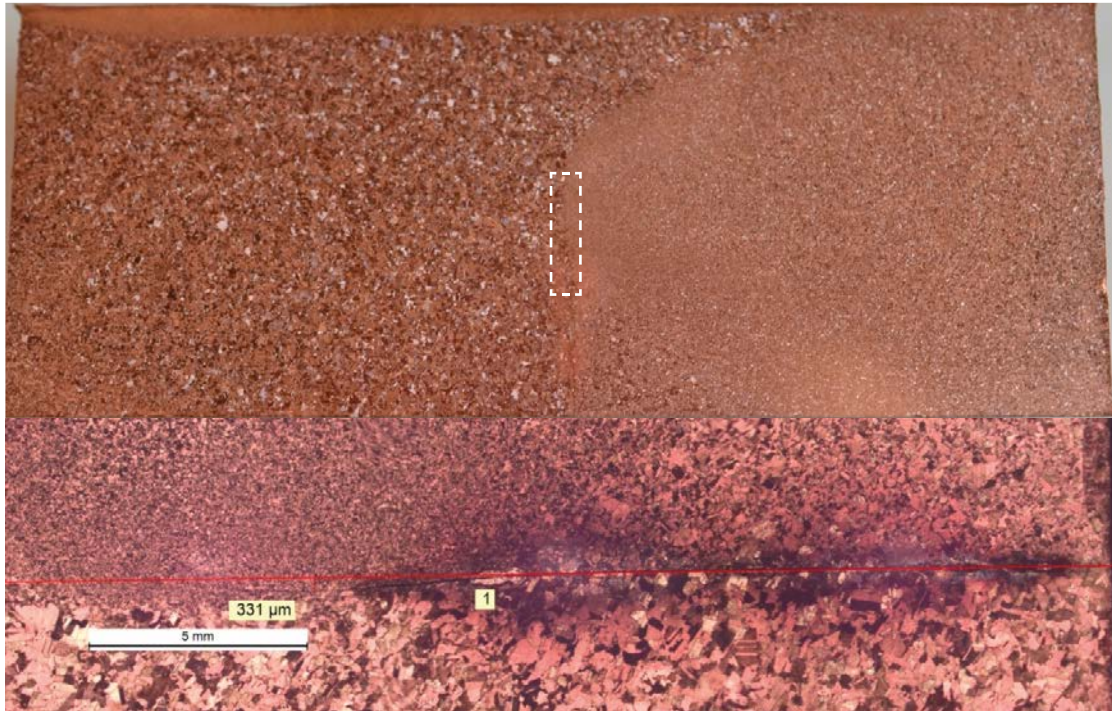


Figure 5-11. Macro sample from weld 612. The top picture shows the weld zone on the right hand side, while the bottom picture shows a zoom of the white dashed box (rotated 90° counter clockwise). A maximum depression of the vertical joint line of 0.331 mm was measured.

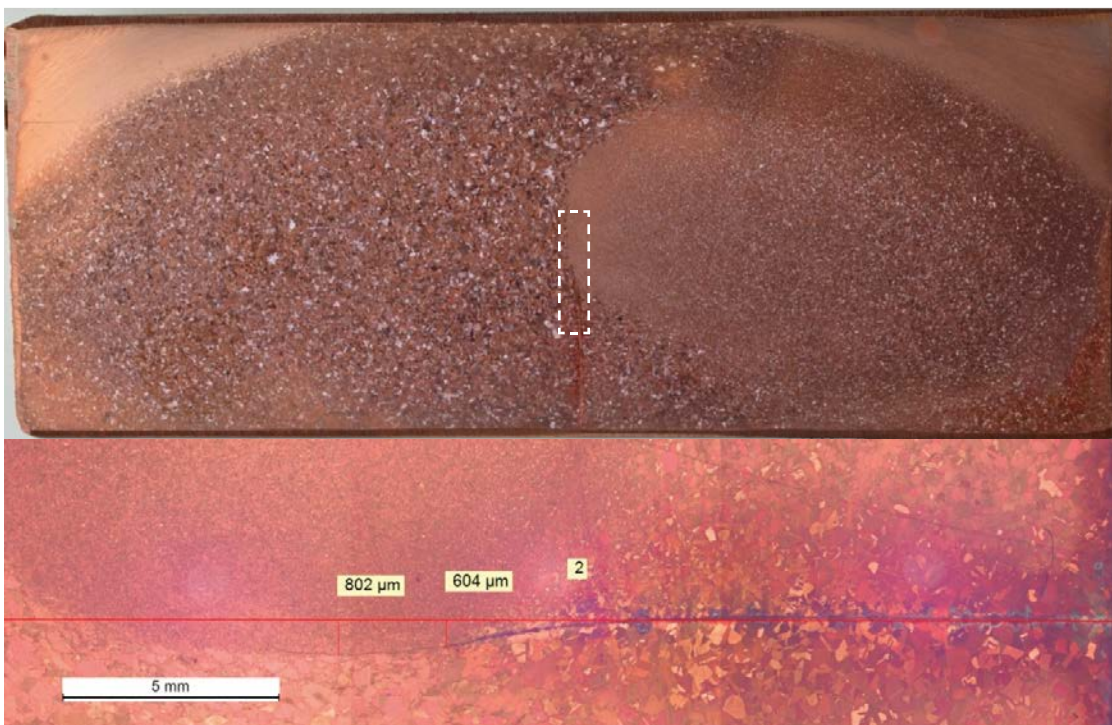


Figure 5-12. Macro sample from weld 640. The top picture shows the weld zone on the right hand side, while the bottom picture shows a zoom of the white dashed box (rotated 90° counter clockwise). A maximum depression of the vertical joint line of 0.802 mm was measured.

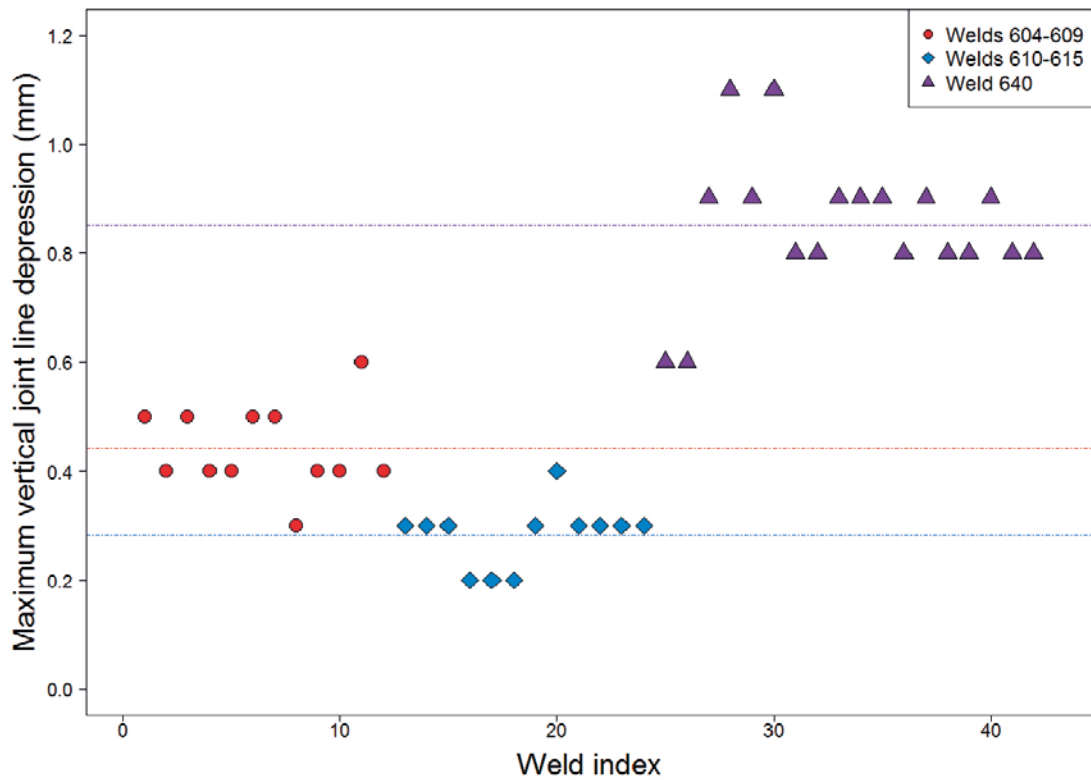


Figure 5-13. Maximum vertical joint line depression in all 42 macro samples from the three lids (114, 115, and 119). The average depressions for each lid are marked with dash-dotted lines in their respective colours (as indicated by the legend).

6 Comparison with welds without depth control

In this section, the depth controlled welds are compared to 18 welds without any active depth control, which will give an indication of the benefits of the depth controller. The data from the welds are collected in Table 6-1. It should be noted that these welds are part of a Design of Experiments series, where different constant axial forces (approximately 75, 80, and 85 kN) have been used. Furthermore, half of the welds (617–619, 623–625, 629–631) have been made with probe temperatures approximately 815 °C (rather than the normal 845 °C) at a point 2° into the joint line sequence. During these 9 welds, the start and downward transition temperatures are lower and, as one would expect, the depth values are also generally lower. The lower probe temperatures are, however, also likely to affect the Shoulder OD temperature, as well as the thermal expansion (and thus also the depth measurements). From previous studies of thermal expansion, it seems fair to expect a difference in thermal expansion (from 815 °C to 845 °C) of approximately 0.03 mm. This gives a relative change of a few percent, and thus is assumed to be small enough to be negligible. The Shoulder OD temperature, on the other hand, seems likely to decrease with both lower heat input and shallower depth. The 9 relevant data points have not yet been altered, but an option would be to calibrate them against a probe temperature of 845 °C. There is also a major benefit of using the lower probe temperature, since the test then has a wider span of depths, making it easier to see how well the different depth sensors and depth indicators model the shoulder footprint depth.

Table 6-1. Data from 18 welds with no active depth control, 2° into the joint line sequence. Diff LVDT is the difference between LVDT1 and LVDT2, Sho temp stands for Shoulder OD temperature (see Figure 1-4), and Fp is an abbreviation for footprint. Means, maximum deviation, and standard deviation are presented in the bottom rows.

Weld ID	Fp width	Fp depth	Laser	LVDT1	LVDT2	Diff LVDT	Sho Temp
616	69.5	2.94	2.06	2.24	2.10	0.14	754.0
617	69.0	2.87	2.19	2.12	1.99	0.13	728.5
618	68.0	2.75	2.11	2.03	1.97	0.06	725.5
619	67.0	2.64	1.98	1.85	1.88	-0.03	686.0
620	68.5	2.81	2.29	2.14	2.15	-0.01	716.5
621	69.5	2.94	2.40	2.33	2.24	0.09	724.0
622	66.0	2.51	1.93	1.75	2.15	-0.40	698.0
623	65.0	2.40	1.83	1.64	2.02	-0.38	670.5
624	66.0	2.51	1.74	1.55	1.81	-0.26	677.0
625	67.5	2.69	1.94	1.78	1.95	-0.17	730.5
626	68.0	2.75	2.16	2.02	2.09	-0.07	747.0
627	69.0	2.87	2.30	2.22	2.03	0.19	748.0
628	67.5	2.69	2.38	2.38	2.39	-0.01	711.5
629	66.0	2.51	1.87	1.68	2.08	-0.40	686.5
630	65.0	2.40	1.97	1.73	2.18	-0.45	680.5
631	64.5	2.34	1.99	1.78	2.08	-0.30	640.0
632	67.5	2.69	2.35	2.11	2.40	-0.29	683.5
633	68.0	2.75	2.49	2.36	2.40	-0.04	693.5
Mean:	67.3	2.67	2.11	1.98	2.11	-0.12	705.6
Max dev:	5.0	0.60	0.75	0.83	0.59	0.64	114.0
St. dev:	1.57	0.19	0.22	0.27	0.17	0.21	31.0

The 18 welds have been made in three different lids and tubes, and the relative hardness of the lids are given in Table 6-2, using the maximum pilot hole forming force. The average hardness values of the lids are: 80.6 kN (welds 616–621), 91.7 kN (welds 622–627), and 103.4 kN (welds 628–633). Comparing these hardness values to those for depth controlled welds, in Table 5-1 (means 97.5 kN, 95.3 kN and 72.4 kN, respectively), it is obvious that weld 640 has been made in the softest lid of the six, welds 616–621 in a soft lid, welds 622–627 in a medium-hard lid, welds 604–609 and 610–615 in hard lids, and welds 628–633 in the hardest lid.

Figure 6-1 is a box plot combined with the data points that make up the boxes. Basically, a box plot gives a rough idea of data distribution. The median value is marked with a thick line in the box, while the first and third quartiles are delineated by the frame of the box. That is, the lower 25 % and upper 25 % of the data are outside the box. A small box thus indicates less variation in the data. The two whiskers (vertical dashed lines with solid horizontal endings) show the extent of the data, except for outliers that are marked with circles. The data points have been added to the plot, and each of these has been colour coded according to the hardness of the lid (see figure legend), as explained in the previous paragraph. All boxes come in pairs, where those on the left show welds without depth control, and those on the right show those with control. The two boxes furthest to the left indicate the Laser measurements at the point where the start sequence begins (time $t = 0$ seconds). The two boxes in the middle show the Laser measurements 2° into the joint line sequence, and the two boxes to the right depict the footprint depth data distribution at the same point.

Figure 6-1 shows that lid hardness is the best factor for determining the depth at the beginning of the start sequence. At a point 2° into the joint line sequence, the hardness appears to have less effect on Laser and footprint depth. That is, welds that are shallow during the dwell sequence have a greater depth increase during the start and downward sequences. Furthermore, welds with active depth control have much less variation than those without control. For the thirteen welds with active depth control, the shoulder depth measured by the Laser sensor varied between 2.19 and 2.40 mm (0.21 mm span) at a point 2° into the joint line sequence, which means a maximum control error of 0.20 mm. The shoulder footprint depth ranged between 2.52–2.86 mm (0.34 mm span). For the eighteen uncontrolled welds, the Laser measurement varied between 1.74 and 2.49 mm (0.75 mm span). The corresponding range for the footprint depth showed a 0.60 mm span. The uncontrolled welds, on the other hand, are greater in number and have a larger variability in lid hardness. Therefore, it seems likely that the depth controller decreases the depth variation, but more tests are needed to show that this conclusion is valid.

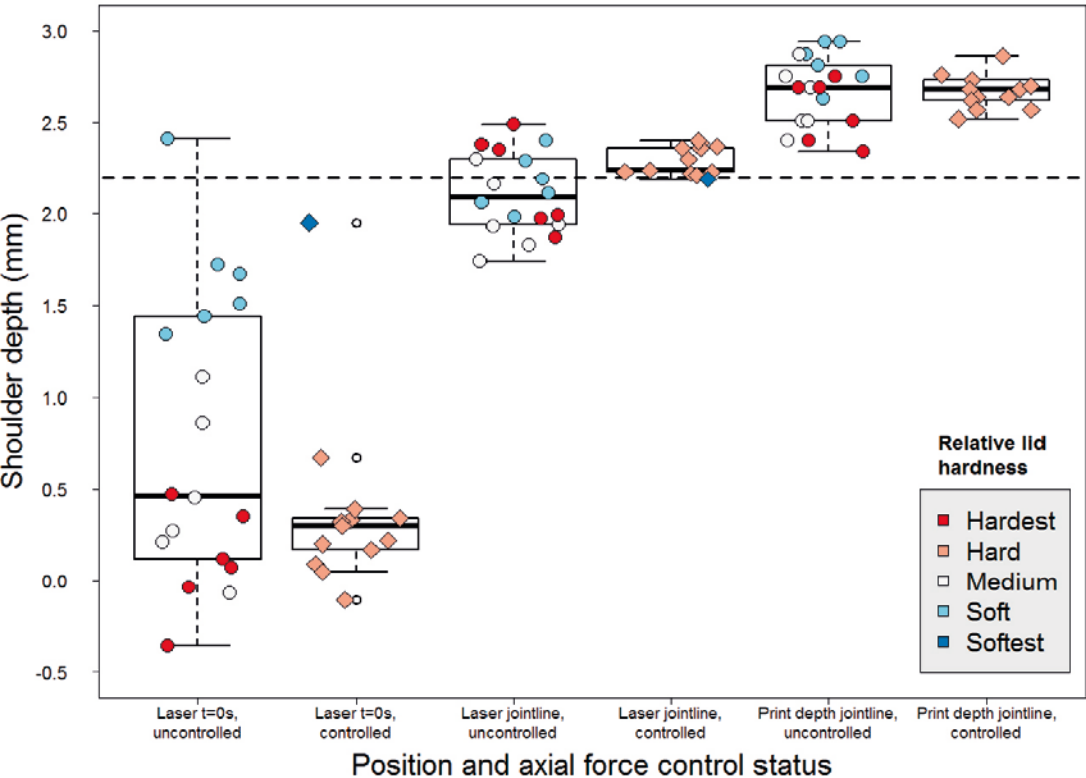


Figure 6-1. Box plot and data points that show the distribution of depth in different welds, at two locations. All boxes come in pairs, where the left box shows welds without control and the right box shows those with control. The colours of the markers are related to the hardness of the lids that the welds were made in (see legend for colour codes). The Laser depth reference point is marked with a dashed horizontal line in the plot.

Table 6-2. Lid hardness in welds 616–633, measured by the maximum axial force (kN) during pilot hole forming. These welds were made in three lids (marked by different colours) without depth control.

Weld ID	616	617	618	619	620	621
Hardness	73.7	81.3	83.3	82.4	81.8	80.9
Weld ID	622	623	624	625	626	627
Hardness	94.1	95.5	87.3	89.2	86.8	97.3
Weld ID	628	629	630	631	632	633
Hardness	102.8	105.3	103.2	104.0	104.4	100.8

The next question to be answered is how well the different depth sensors and indicators can model the actual depth. For this purpose, each signal has been used to model the shoulder footprint depth (2° into the joint line sequence) as estimated from the shoulder footprint width. Figures 6-2 to 6-6 show plots of footprint depth versus Laser, LVDT1, LVDT2, LVDT difference (Diff LVDT), and Shoulder OD temperature, respectively. The red crosses show the welds with depth control; in most cases, these obviously do not have enough variation to provide a decent model. When they are combined with the uncontrolled welds (in black circles), however, it is possible to derive much more reliable models. Linear regression models with one variable have been derived (minimum least squares modelling in the programming language R) and plotted with blue dashed lines in the figures. Their respective 95 % confidence intervals are marked with grey regions. This analysis gives the following models (in mm):

$$\text{Footprint Depth} = 0.42 \cdot \text{Laser} + 1.75, \quad (6-1)$$

$$\text{Footprint Depth} = 0.47 \cdot \text{LVDT1} + 1.72, \quad (6-2)$$

$$\text{Footprint Depth} = 0.094 \cdot \text{LVDT2} + 2.46, \quad (6-3)$$

$$\text{Footprint Depth} = 0.62 \cdot \text{Diff LVDT} + 2.76, \quad (6-4)$$

$$\text{Footprint Depth} = 0.0050 \cdot \text{Shoulder OD Temperature} - 0.86. \quad (6-5)$$

In addition to these one variable models, two multiple linear regression models have been derived, a two variable model with Shoulder OD Temperature and LVDT measurement difference as predictors:

$$\text{Footprint Depth} = 0.0036 \cdot \text{Shoulder OD Temperature} + 0.35 \cdot \text{Diff LVDT} + 0 \quad (6-6)$$

and a three variable model with Shoulder OD Temperature, LVDT measurement difference, and Laser measurement as the predictors:

$$\text{Fp.D.} = 0.0033 \cdot \text{Shoulder OD Temp.} + 0.31 \cdot \text{Diff LVDT} + 0.16 \cdot \text{Laser} + 0.064. \quad (6-7)$$

These models are the two and three variable models with the highest accuracy among all linear regression models that can be created by any two or three of the five measurements. Table 6-3 summarizes measures of the models (on training data) that indicate both how significant the model relationships are and how accurately the models describe the footprint depth. The F-statistic (James et al. 2013) can be derived to measure the significance of the hypothesis that there is a relationship between the variables. An F-statistic value much larger than 1 indicates a high probability that a relationship exists. The accuracy of the model can be assessed using the R² metric (James et al. 2013), which takes on a value between 0 and 1. The R² metric is attractive, as it explains how much of the predicted variable variation is explained by the model. A model with its R² value close to 1 will thus explain almost all variability, and the relationship is therefore strong. On the other hand, a model with an R² value close to 0 explains very little of the result's variability. Figure 6-7 shows box plots of the prediction errors for all seven models (together with the data points). Figure 6-8 shows normal quantile-quantile probability plots for the same models, showing that the residuals are approximately normal distributed in all seven cases. K-fold cross validation (James et al. 2013) has also been used to verify the quality of the models, but this analysis is not included in this report.

Table 6-3. F-statistics and R² statistics for the seven linear regression models.

Model:	(6-1)	(6-2)	(6-3)	(6-4)	(6-5)	(6-6)	(6-7)
F-statistic	11.1	23.2	0.39	31.4	55.4	45.7	35.9
R ² statistic	0.28	0.46	0.014	0.54	0.66	0.78	0.81

The F-statistics in Table 6-3 show that valid relationships appear to exist in all cases except model (6-3) (LVDT2), which also has a very low R² measure. Interestingly, among all one variable models, the Shoulder OD temperature model seems best at predicting the footprint depth. Even the LVDT difference seems to be better at predicting this depth than the ordinary depth sensor signals. However, it may be that the shoulder footprint width depends on the relative diameter difference between the lid and the tube. In that case, the shoulder depth may not be entirely well predicted by the estimated footprint depth, since it fails to consider the relative material thickness. That would explain why the Shoulder OD temperature and LVDT difference work best for modelling the estimated footprint depth.

Of the three shoulder depth sensors, LVDT1 seems to give the best predictions of the footprint depth. Based on this observation and the Laser signal measurement noise (see Figure 1-9), it seems reasonable to use the LVDT1 sensor for the controller feedback signal. The Laser signal can be used as a back-up in case of an LVDT1 sensor failure (as in weld 614), as can the Shoulder OD temperature value.

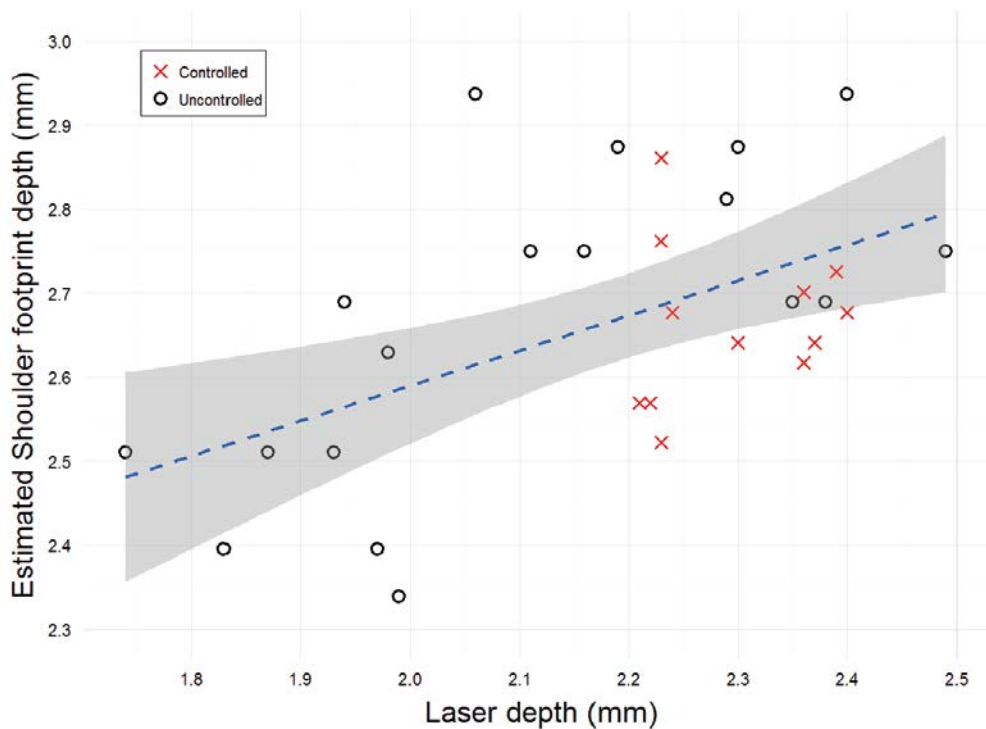


Figure 6-2. Linear regression of footprint depth using the Laser as predictor. The linear model (6-1) is marked with a dashed blue line, with its 95 % confidence interval in grey. Depth controlled welds are shown with red crosses and welds without depth control with black circles.

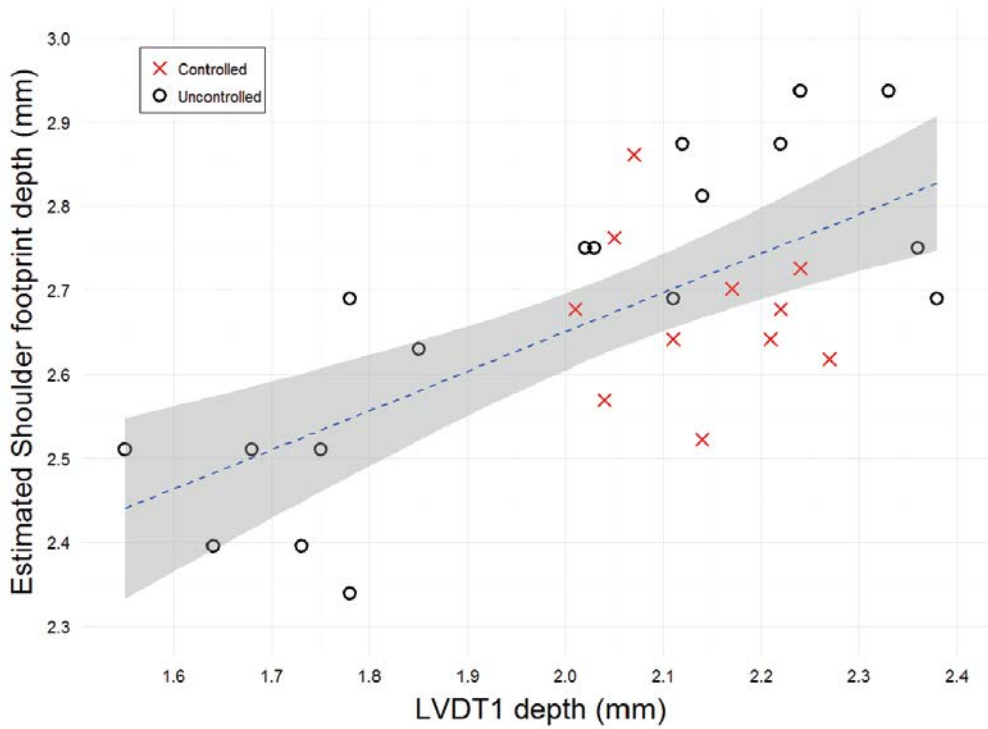


Figure 6-3. Linear regression of footprint depth using LVDT1 as predictor. The linear model (6-2) is marked with a dashed blue line, with its 95 % confidence interval in grey. Depth controlled welds are shown with red crosses and welds without depth control with black circles.

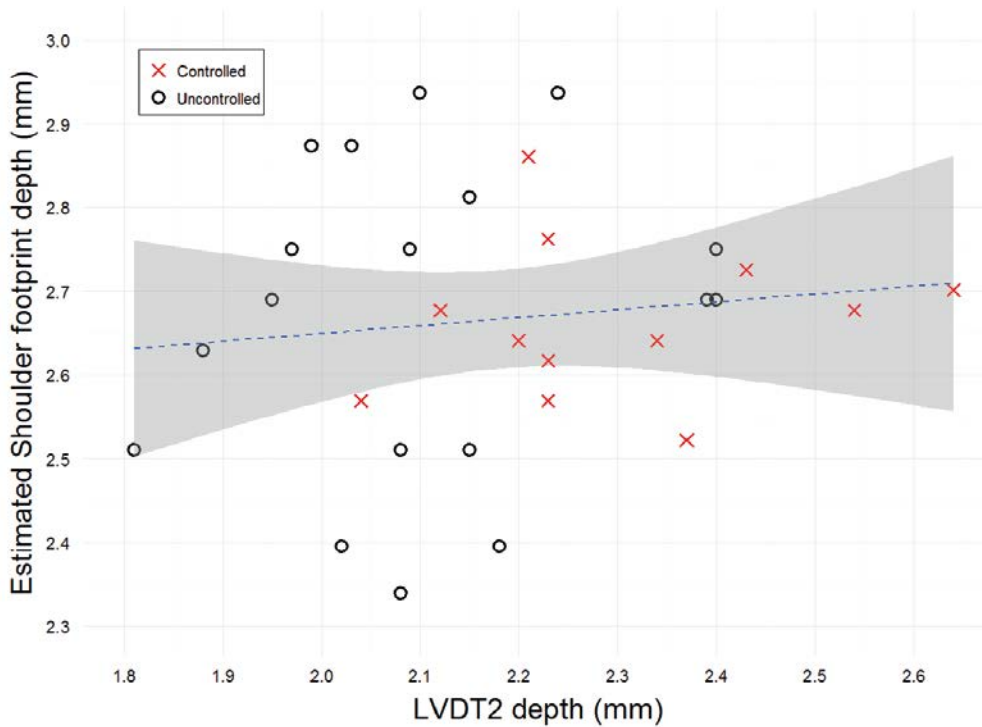


Figure 6-4. Linear regression of footprint depth using LVDT2 as predictor. The linear model (6-3) is marked with a dashed blue line, with its 95 % confidence interval in grey. Depth controlled welds are shown with red crosses and welds without depth control with black circles.

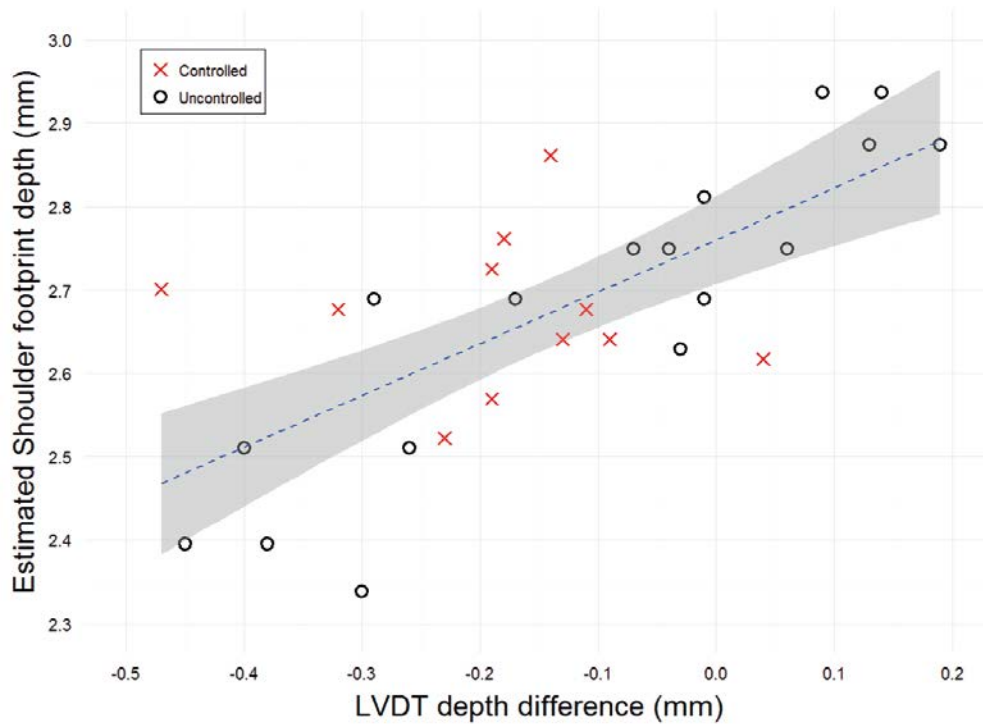


Figure 6-5. Linear regression of footprint depth using the LVDT difference as predictor. The linear model (6-4) is marked with a dashed blue line, with its 95 % confidence interval in grey. Depth controlled welds are shown with red crosses and welds without depth control with black circles.

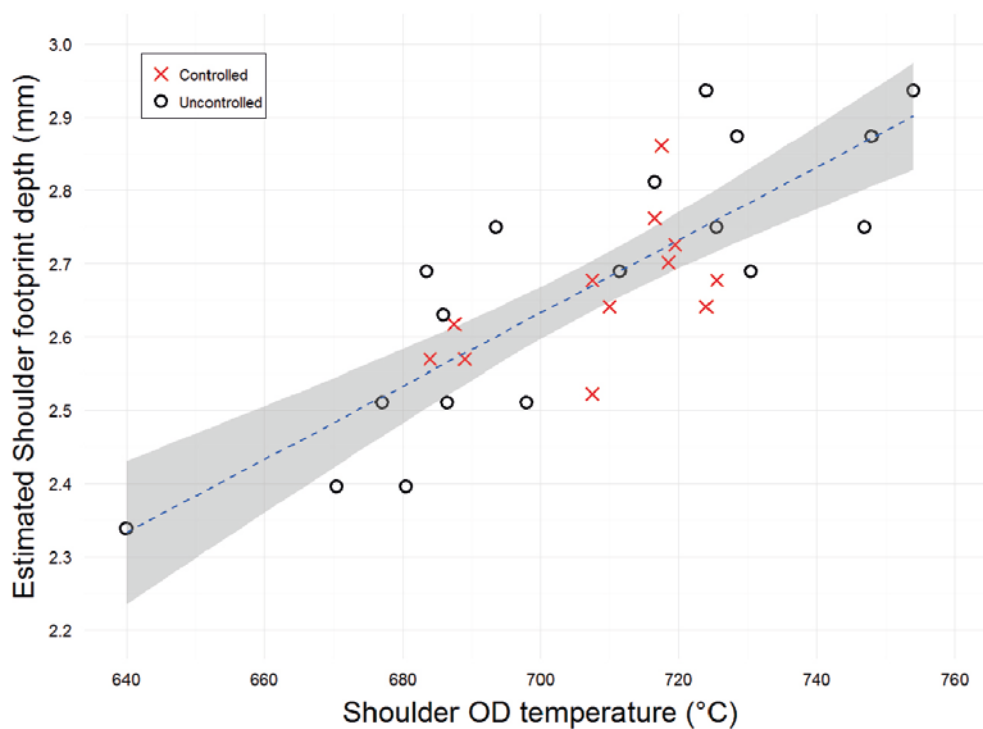


Figure 6-6. Linear regression of footprint depth using shoulder OD temperature as predictor. The linear model (6-5) is marked with a dashed blue line, with its 95 % confidence interval in grey. Depth controlled welds are shown with red crosses and welds without depth control with black circles.

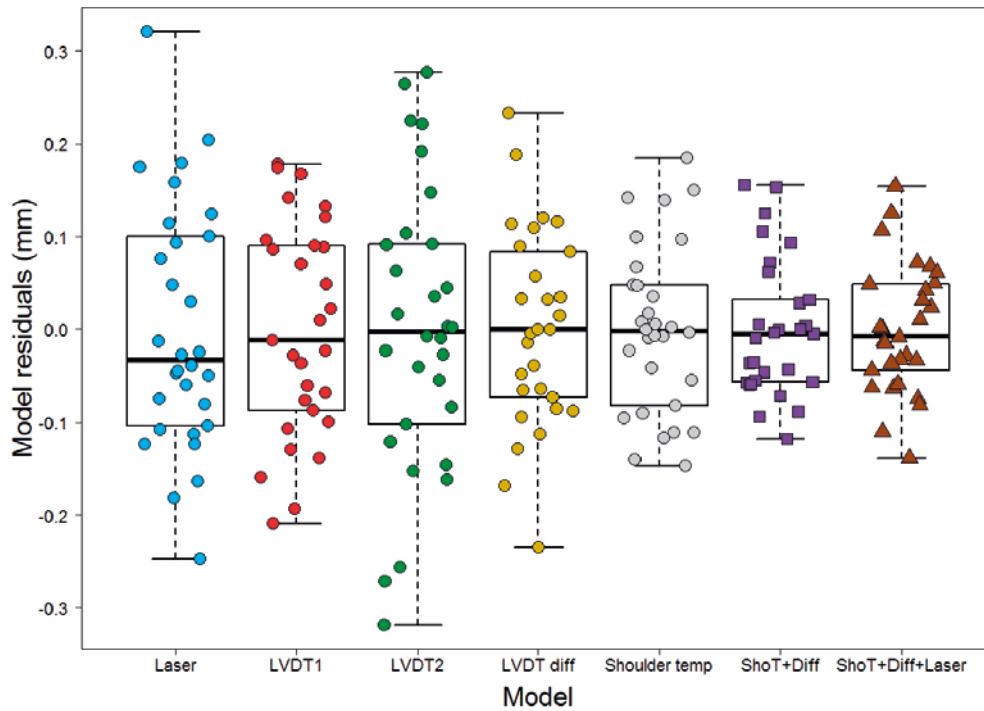


Figure 6-7. Box plot of the different footprint depth model residuals using seven different models (6-1) to (6-7). LVDT diff (or just Diff) denotes the difference between the two LVDT sensors, while ShoT (and Shoulder temp) denotes the Shoulder OD temperature. The models are in the same order as in the body text. The residuals themselves are also plotted, with different symbols for the two models that depend on more than one variable.

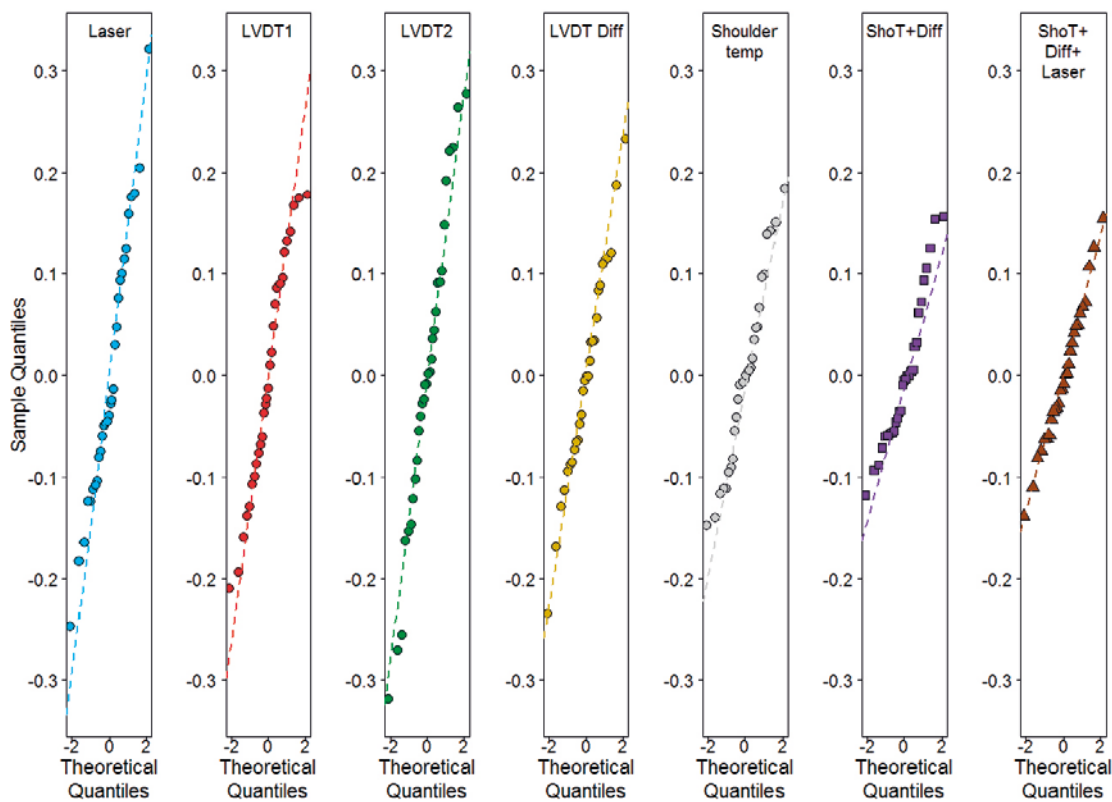


Figure 6-8. Normal quantile-quantile probability plot of the different footprint depth model residuals using seven different models (6-1) to (6-7). LVDT diff (or just Diff) denotes the difference between the two LVDT sensors, while ShoT (and Shoulder temp) denotes the Shoulder OD temperature. The models are in the same order as in the body text.

7 Conclusions

In concluding this report, the questions from chapter 4 are reviewed and answered to the extent possible from the current state of knowledge concerning the depth controller.

1. Which sensors can be used to estimate the depth? How accurately can the depth be estimated?

As we have seen in the previous section, the Laser, LVDT1, the difference between the LVDT measurements, and the Shoulder OD temperature can all be used to predict the shoulder depth in terms of the estimated footprint depth. The LVDT2 sensor has only a weak relation (if any) to the footprint depth. The Shoulder OD temperature is the most accurate for modelling the shoulder footprint, with residuals around ± 0.15 mm. Of those sensors that can be used by the controller, the LVDT1 sensor has the highest accuracy, at about ± 0.20 mm.

2. Which sensor(s) should be fed back to the controller?

From the findings of this study, it is suggested that the LVDT1 sensor be used for the feedback signal in the depth controller. It is the most accurate sensor in predicting the shoulder footprint depth, and it does not suffer from measurement noise like the Laser signal does.

3. What shoulder depth reference should be used?

The verification welds use a reference of 2.2 mm for the depth when measured by the Laser sensor. The macro samples show this to be a reasonable reference, since none of the samples show any signs of either joint line hooking or remnants. The length of the probe varies between 50.6–51.1 mm over these welds, which suggests that the process window for the depth is relative large. In other words, it is possible to produce welds without discontinuities if the depth is within a reasonable distance from the reference. However, more tests should be done in lids and tubes with softer copper to verify that these welds do not risk going too deep and to define the process window for the shoulder depth.

The depth reference also seems fine with regard to flash formation. However, the cause of the flash needs to be better investigated. While shoulder depth plays a role, it also seems like a large relative diameter difference between the lid and the tube has a causative effect.

If the controller feedback sensor is changed to LVDT1, the reference needs to be updated as well. On average, the Laser signal is approximately 0.15 mm greater than the LVDT1 sensor (2° into the joint line), so a reasonable reference for LVDT1 would be 2.05 mm, or maybe a little larger, to allow the controller to work within its saturation limits more frequently.

4. Is it possible to control the depth with sufficient accuracy? What limitations are there?

Once again, this seems promising when looking at the reports on the 38 macro samples, which show no indication of joint line hooking over the three lids/rings that have been tested. However, additional welds in lids made by various manufacturing techniques are needed to ensure that welds without joint line hooking can be reliably produced.

5. What alternative strategies can be used to control the depth?

So far, the current strategy seems to be sufficient. However, if future welds show that it is necessary to control the depth more accurately, for example for softer lids, it seems reasonable to try adding depth control during the dwell sequence. This could include control of both the dwell/heat-up time and the depth.

6. How can a fail-safe depth control strategy be implemented?

A first approach might be to implement a switch between feedback signals to the depth controller. If the LVDT1 signal is lost, the Laser seems best suited as a back-up signal. Another possibility would be to also use the Shoulder OD temperature measurements as a feedback signal. LVDT2 could also be used, but the lid/tube transition needs to be accounted for.

Sensor functionality can be checked in almost the same way as in the safety system for the temperature controller, that is, by checking inter-sample differences and judging whether they are reasonable.

References

SKB's (Svensk Kärnbränslehantering AB) publications can be found at www.skb.com/publications. SKBdoc-documents will be submitted upon request to document@skb.se.

Cederqvist L, 2011. Friction stir welding of copper canisters using power and temperature control. PhD thesis. Lund University, Sweden.

Cederqvist L, Garpinger O, Hägglund T, Robertsson A, 2012a. Cascade control of the friction stir welding process to seal canisters for spent nuclear fuel. *Control Engineering Practice* 20, 35–48.

Cederqvist L, Garpinger O, Nielsen I, 2012b. Control of temperature, power input and tool depth during FSW of copper canisters. In *Proceedings of 9th International Symposium on Friction Stir Welding*. Huntsville, Alabama, 15–17 May 2012. Cambridge: TWI, 328–334.

Garpinger O, Hägglund T, 2008. A software tool for robust PID design. *IFAC Proceedings Volumes* 41, 6416–6421.

Hjertsén D, 2016a. Macro samples: FSW114 and FSW115. Exova Test Report PRO16-0637. Linköping. SKBdoc 1555382 ver 1.0, Svensk Kärnbränslehantering AB.

Hjertsén D, 2016b. Macro samples: FSW110 and FSW119. Exova Test Report PRO16-0971. Linköping. SKBdoc 1555381 ver 1.0, Svensk Kärnbränslehantering AB.

James G, Witten D, Hastie T, Tibshirani R, 2013. *An introduction to statistical learning: with applications in R*. New York: Springer.

Nielsen I, Garpinger O, Cederqvist L, 2013. Simulation based evaluation of a nonlinear model predictive controller for friction stir welding of nuclear waste canisters. In *Proceedings of the 2013 European Control Conference*, Zürich, Switzerland, 17–19 July 2013.

Thegerström C, 2004. Down to earth and below: Sweden's plans for nuclear waste. *IAEA Bulletin* 46, 36–38.

Thomas W M, Nicholas E D, Needham J C, Murch M G, Temple-Smith P, Dawes C J, 1991. Friction stir butt welding. International Patent Application No. PCT/GB92/02203.

Åström K J, Hägglund T, 2006. *Advanced PID control*. Research Triangle Park, NC: ISA – The Instrumentation, Systems, and Automation Society.

A CO-OPERATION REPORT BETWEEN SVENSK KÄRNBRÄNSLEHANTERING AB AND POSIVA OY

SKB's and Posiva's programmes both aim at the disposal of spent nuclear fuel based on the KBS-3 concept. Formal cooperation between the companies has been in effect since 2001. In 2014 the companies agreed on extended cooperation where SKB and Posiva share the vision "Operating optimised facilities in 2030". To further enhance the cooperation, Posiva and SKB started a series of joint reports in 2016, which includes this report.